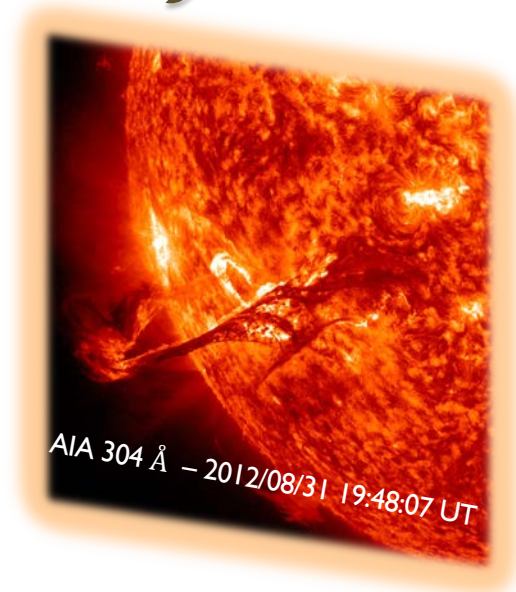


Overview of Eruptive Events Occurring in the Solar Atmosphere

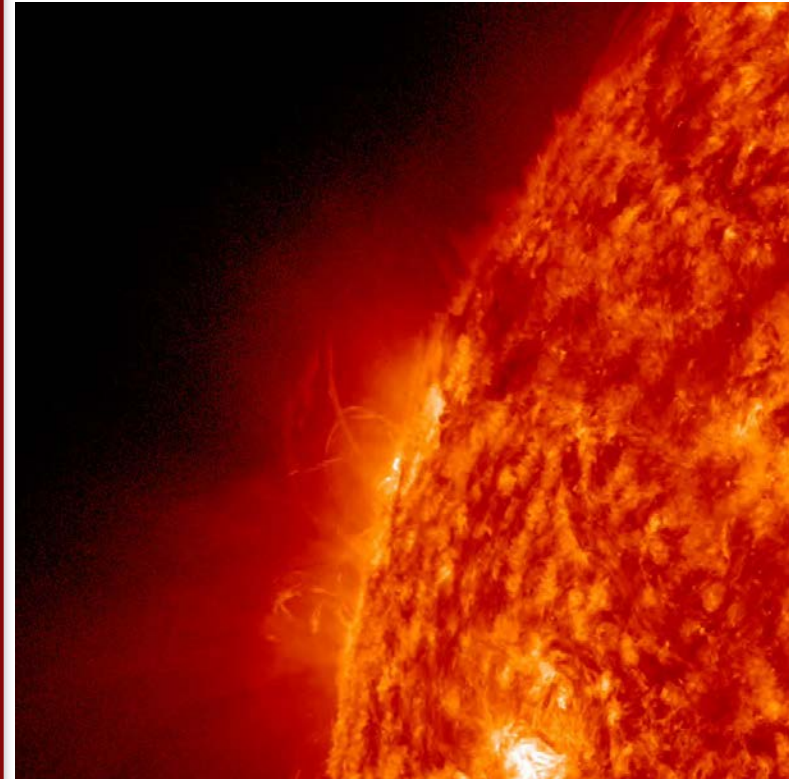
Francesca Zuccarello
Dipartimento di Fisica e Astronomia
'Ettore Majorana'
Università di Catania



The different spatio-temporal scales of the solar magnetism
11 - 15 April 2022
L'Aquila, Italy
International School of Space Science

Plan of the Talk

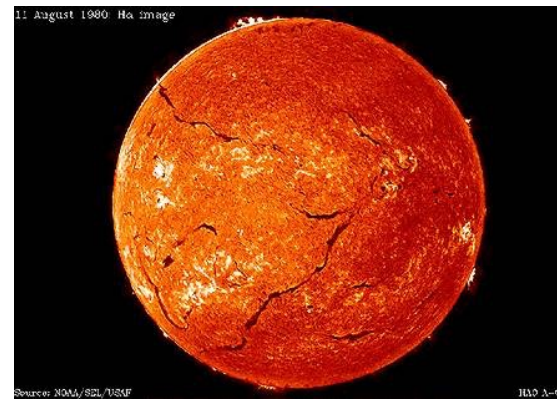
- ✧ Eruptive phenomena
- ✧ Coronal conditions and magnetic reconnection
- ✧ Filaments/Prominences
- ✧ Flares
 - ✧ Observations at different wavelengths
 - ✧ How eruptions can be triggered
 - ✧ How they affect the solar atmosphere
- ✧ CMEs
- ✧ Observing eruptive events with the new generation of solar telescopes



AIA 304 Å – 2012/12/31

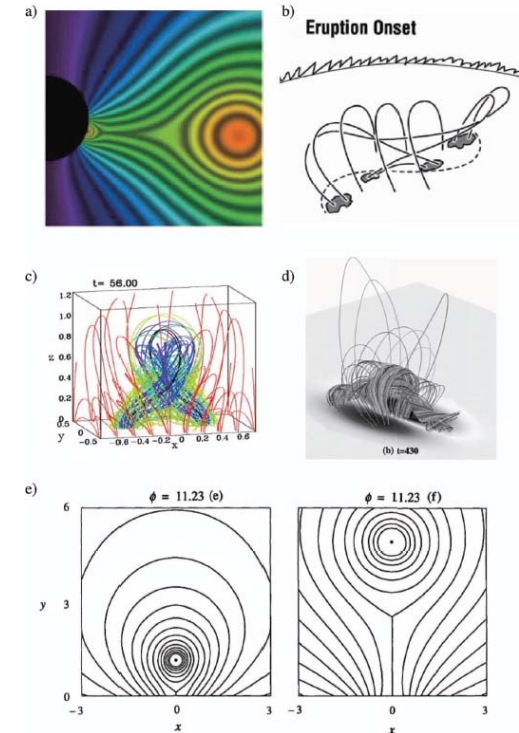
Eruptive phenomena: prominence/filament eruption

Filament activation is a precursor of approaching flare activity.



Filaments outside ARs can erupt and give rise to CMEs

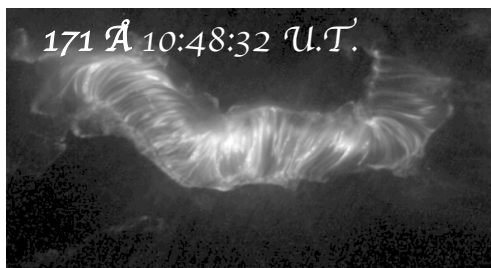
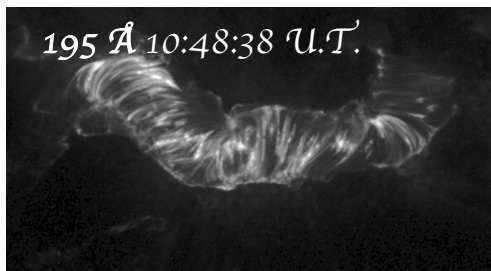
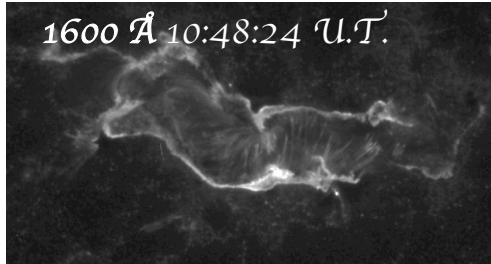
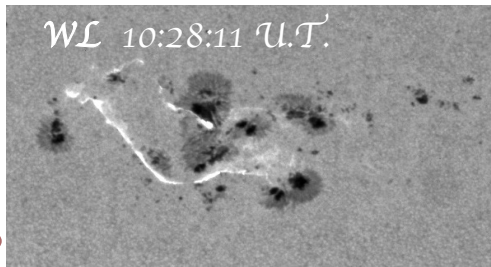
Chromosphere - Corona



Models for the eruption of a flux rope. (a) Flux-cancellation ([Linker et al., 2003](#)). (b) Tether-cutting ([Moore et al., 2001](#)). (c) Kink instability ([Fan & Gibson, 2003](#)). (d) Flux cancellation ([Amari et al., 2000](#)). (e) Loss-of-equilibrium ([Forbes & Isenberg, 1991](#)).

Eruptive phenomena: flares

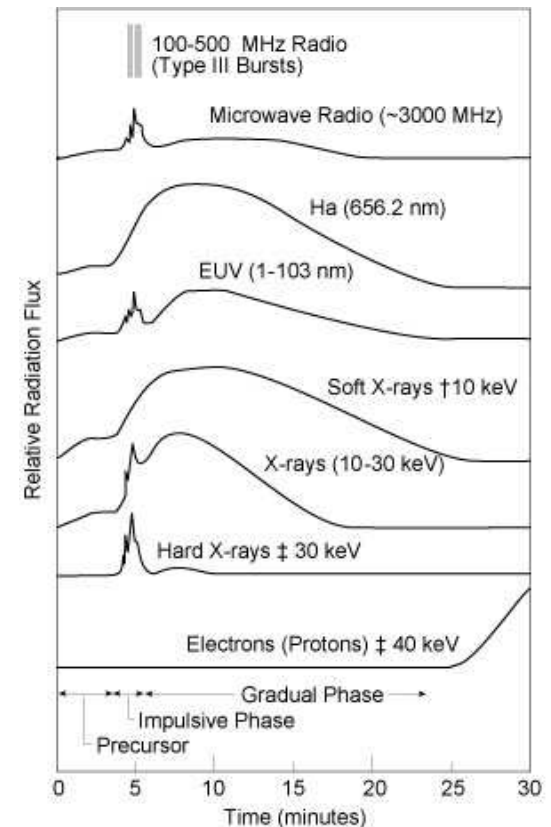
Flares are magnetically driven phenomena that can involve all the atmospheric layers (and beyond ...)



They are characterized by a violent and sudden release of energy, of $\sim 10^{28} - 10^{32}$ erg, that can last for some tens of minutes or hours and can involve emission in the whole electromagnetic spectrum.

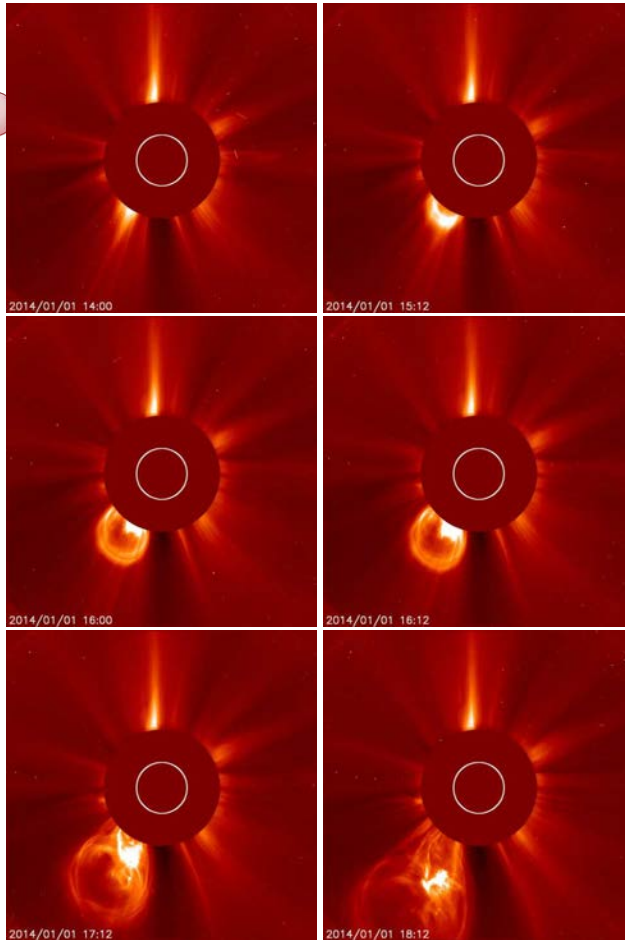
Magnetic energy is converted into particle energy, heat, waves, e.m. radiation and plasma motion.

Photosphere -
Chromosphere -
Corona



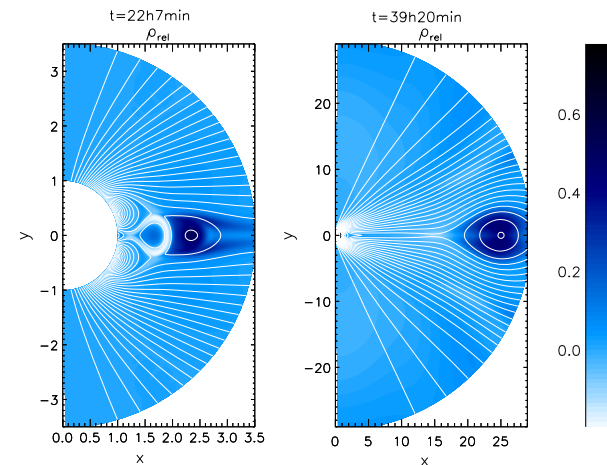
Eruptive phenomena: CMEs

CME observed by LASCO-C3.



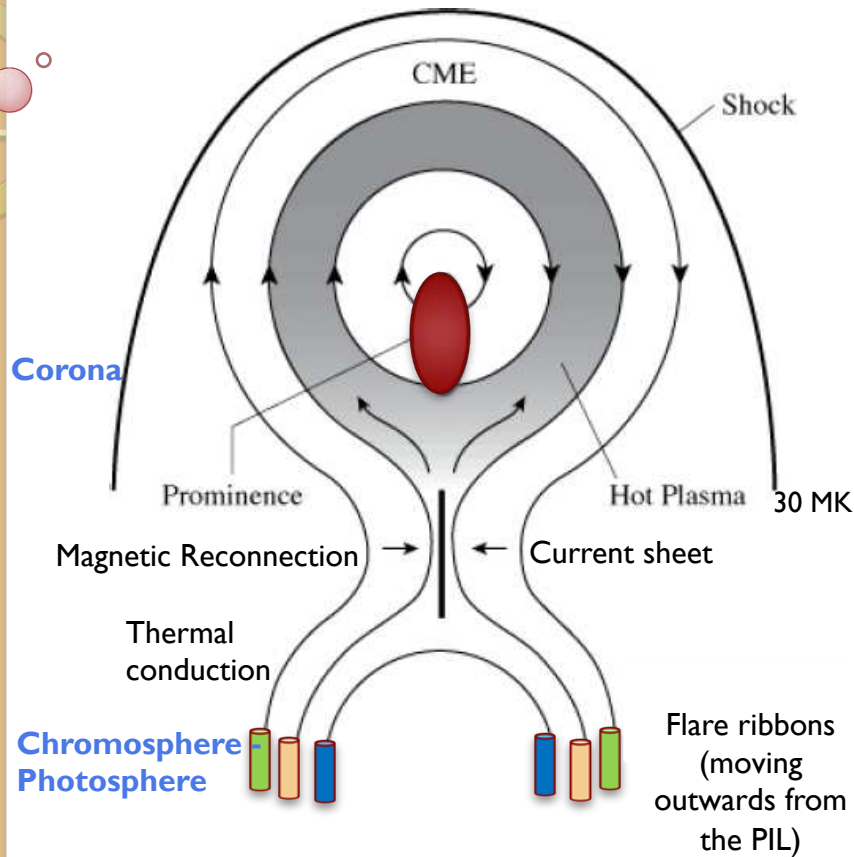
For an X-class event the flare radiation and the CME kinetic energy can have comparable magnitudes (10^{32} erg).

CMEs: expulsion of mass of the order of $10^{14} - 10^{16}$ g, with $v \sim 10^3$ km/s, involving an energy release of $\sim 10^{28} - 10^{32}$ erg. The departure of coronal plasma can produce dimmings in the corona.



Snapshots of the relative density and of the magnetic field lines in the simulation of [Zuccarello et al. \(2009\)](#).

Corona



The 2D standard model, with the locations of the rising filament / prominence, the current sheet, the flare ribbons ($H\alpha$, UV and EUV) the footpoints (HXR and WL) and the CME.

2

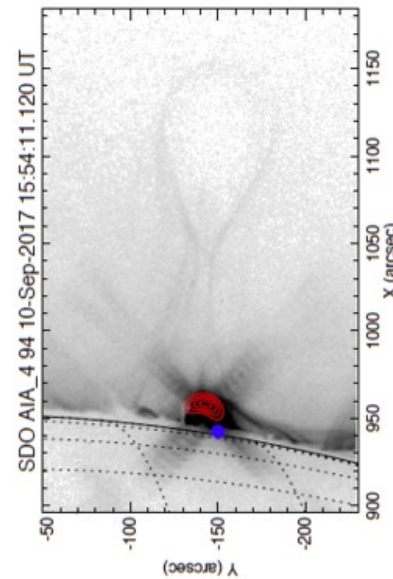
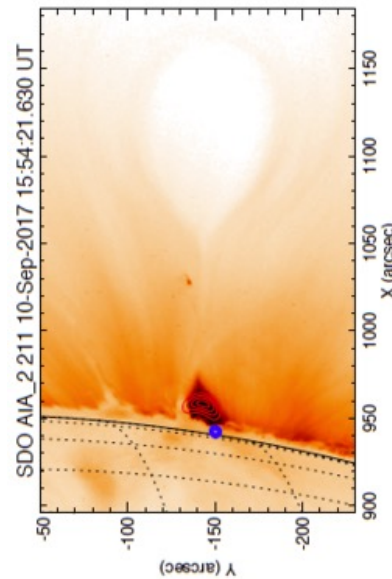
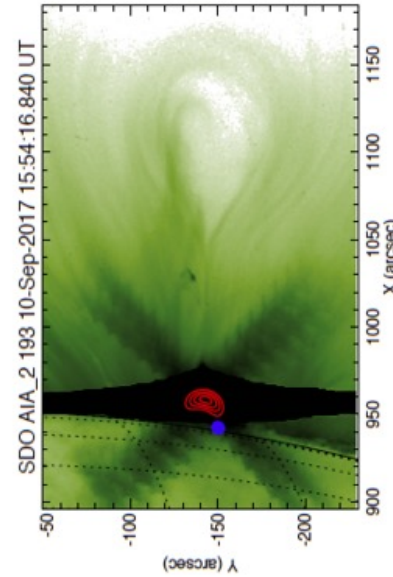
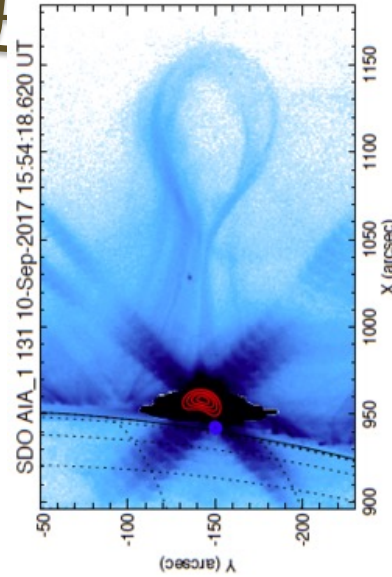


Image rotated 90° counterclockwise.

Solar Coronal Plasma

- Corona: hot, low density plasma (relatively to solar interior)
 - $T \sim 10^6$; $n_e \sim 10^9 \text{ cm}^{-3}$; $P \sim 1 \text{ Dyne cm}^{-2}$
 - Plasma fully ionized

- Magnetohydrodynamics (MHD) approximation

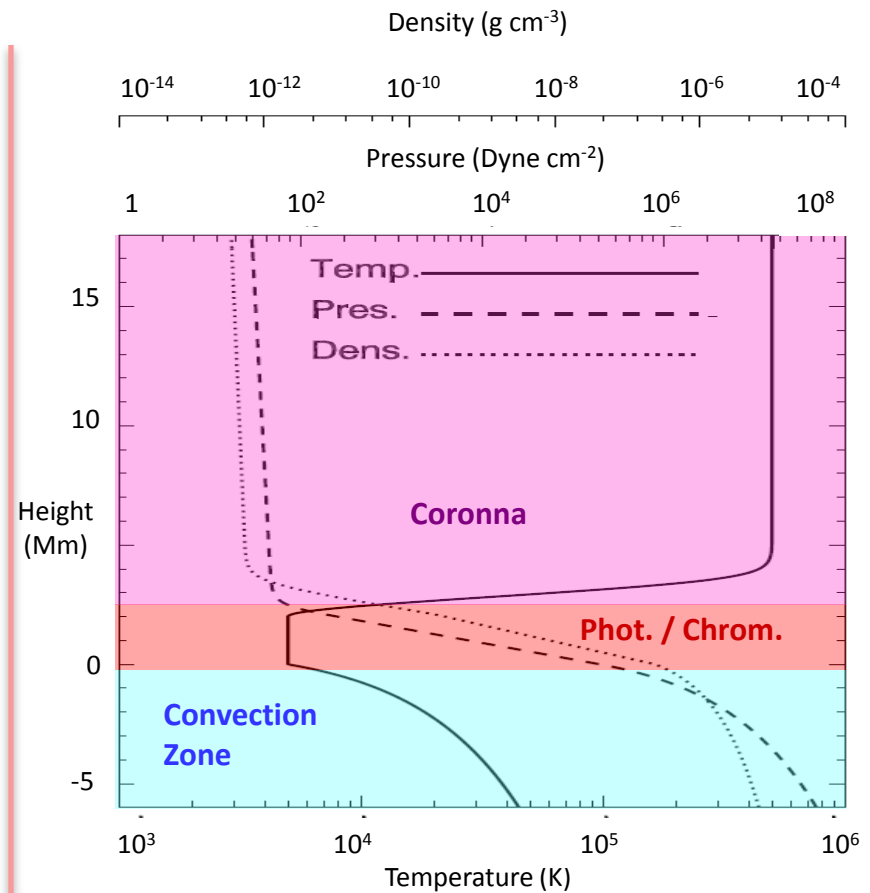
- Fluid approximation
- Non relativistic scales ($v_0 \ll c$)
 - Electric currents are induced by the magnetic field : Ampère Law

$$\mu_0 \mathbf{J} = \nabla \times \mathbf{B}.$$

- Quasi-neutrality

- For length scale \gg Debye length, $\sim 1 \text{ cm}$ in the corona

$$\lambda_D = \sqrt{\frac{\epsilon_0 k_B T_e}{n_e q_e^2}}$$



(adapted from E. Pariat
Presentation - Vulcano 2012)

Ideal MHD Approximation

- Electric field in a moving plasma: $\underline{E}' = \underline{E} + \underline{v} \times \underline{B}$
- Resistive Ohm Law ($\underline{E}' = \eta \underline{j}$) + Ampère law ($\mu_0 \underline{j} = \nabla \times \underline{B}$) + Faraday law $\nabla \times \underline{E} = - \frac{\partial \underline{B}}{\partial t}$

- MHD induction equation

$$\frac{\partial \underline{B}}{\partial t} = \eta \nabla^2 \underline{B} + \nabla \times (\underline{v} \times \underline{B})$$

- Magnetic Reynolds number:

- $R_m \gg 1$: Ideal MHD
- $R_m \ll 1$: Resistive MHD

$$R_m = \frac{V_0 L_0}{\eta}$$

- Solar Corona:

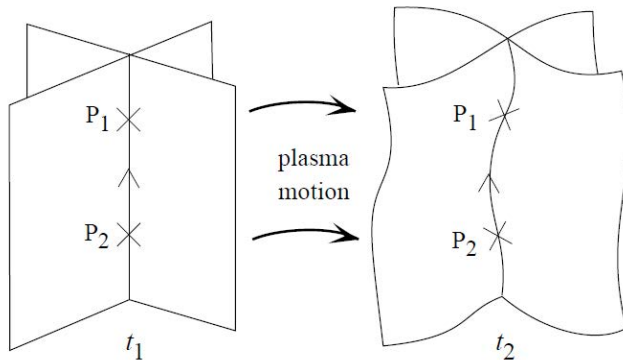
- $V_0 \sim 1 \text{ km s}^{-1}$, $\eta \sim 10^{-3} \text{ m}^2 \text{ s}^{-1}$, $L_0 \sim > 10 \text{ km}$
- **$R_m > 10^4$: ideal MHD is a very good approximation of the solar corona**

Frozen-in Flux in Ideal MHD

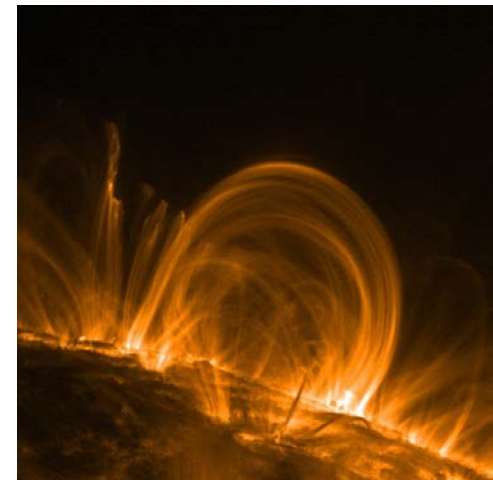
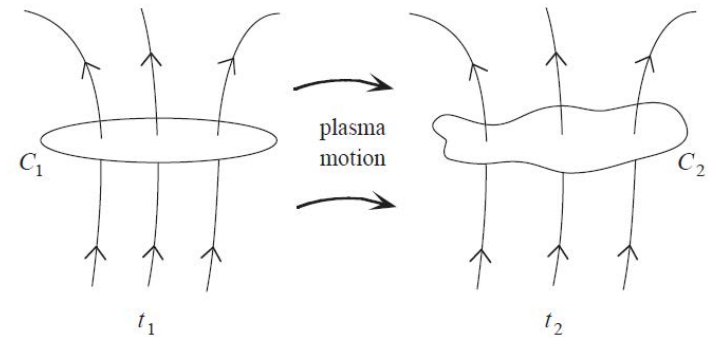
- Ideal MHD induction equation:
- **Magnetic flux conservation: the flux through any closed co-moving surface is conserved**

$$\frac{d}{dt} \int_S \mathbf{B} \cdot d\mathbf{S} = \int_S \frac{\partial \mathbf{B}}{\partial t} \cdot d\mathbf{S} + \int_C \mathbf{B} \cdot \mathbf{v} \times d\mathbf{s}.$$

- **Frozen flux: plasma & magnetic field line are frozen together:**
- → Magnetic field lines are physical objects
- **Connectivity conservation: two plasma elements lying initially on a field line will always do so**
- → field line cannot change its topology / connectivity



$$\frac{\partial \mathbf{B}}{\partial t} = \nabla \times (\mathbf{v} \times \mathbf{B})$$



Plasma β

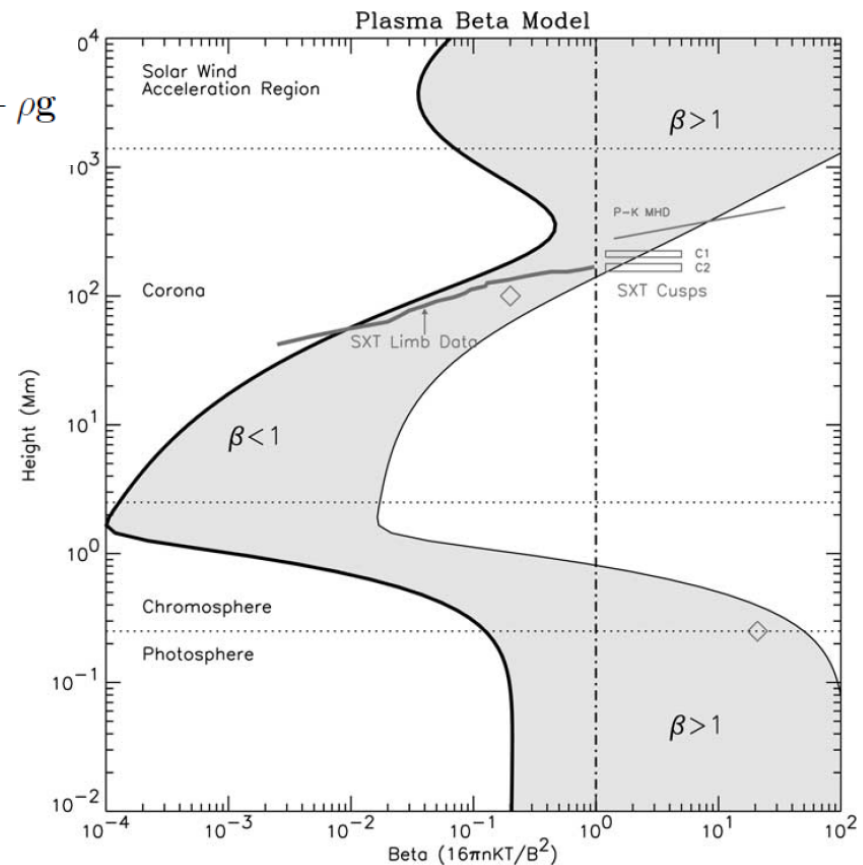
- MHD Momentum equation:

$$\rho \frac{\partial \mathbf{v}}{\partial t} + \rho(\mathbf{v} \cdot \nabla)(\mathbf{v}) = -\nabla P + \frac{1}{\mu}(\nabla \times \mathbf{B}) \times \mathbf{B} + \rho \mathbf{g}$$

- Plasma beta:

$$\beta = \frac{2\mu_0 P}{B^2}$$

- $\beta \gg 1$: thermodynamic dominates the plasma dynamics
- $\beta \ll 1$: magnetic field dominates
- Corona: $\beta \ll 1$
 - **B dominated region: magnetic field fills the whole coronal volume and structure the domain.**
- Sub-photosphere: $\beta > 1$
 - **Plasma dominated: plasma flows advect the magnetic flux tubes**

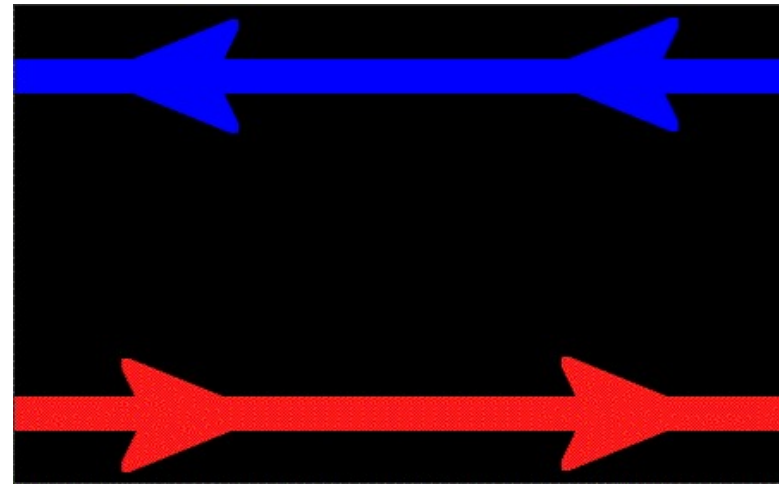


Magnetic Reconnection

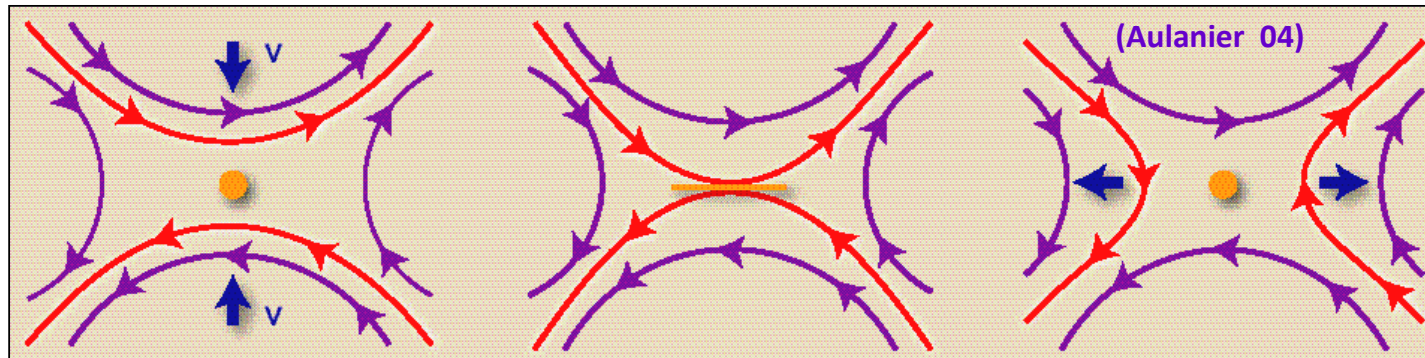
- **Magnetic reconnection is the mechanism that correspond to the local violation of the ideal MHD conditions**
- MHD induction equation
- Magnetic Reynolds number:
 - $R_m \gg 1$: Ideal MHD ; $R_m \ll 1$: Resistive MHD
- Solar Corona: $V_0 \sim 1 \text{ km s}^{-1}$, $\eta \sim 10^{-3} \text{ m}^2 \text{ s}^{-1}$:
 - $R_m \sim 1$ for $L_0 \sim 1 \text{ m}$: recon. is a VERY localized process relatively to solar scales
- **Magnetic reconnection locally diffuse the plasma and allows a change of connectivity of the field lines**

$$\frac{\partial \mathbf{B}}{\partial t} = \nabla \times (\mathbf{v} \times \mathbf{B})$$

$$\mathcal{R}_m = \frac{V_0 L_0}{\eta}$$



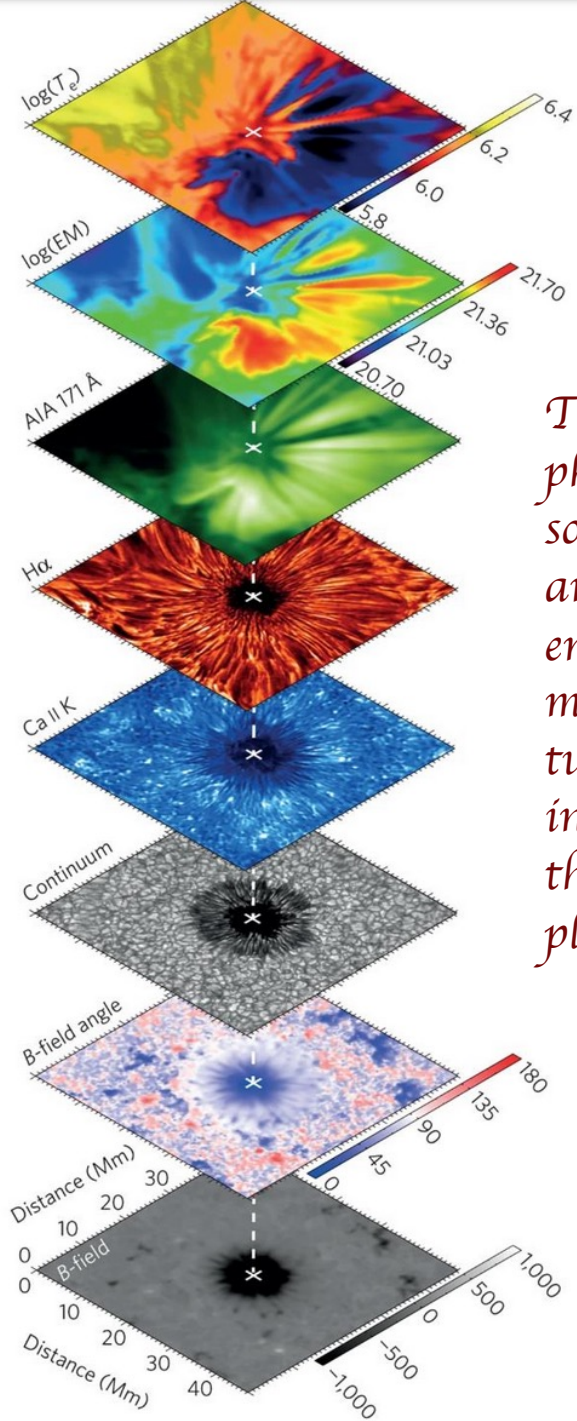
Magnetic Reconnection



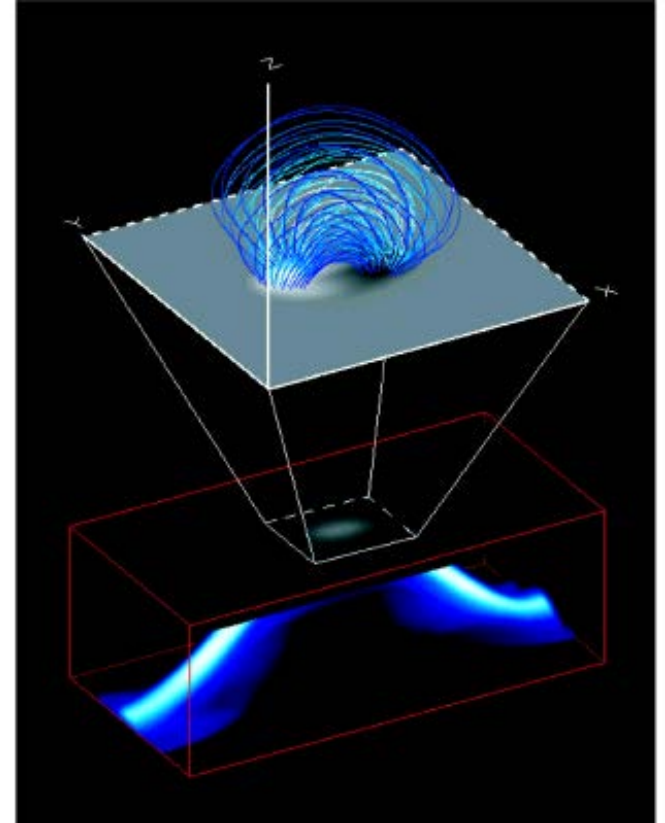
$$\frac{\partial \underline{\mathbf{B}}}{\partial t} = \eta \nabla^2 \underline{\mathbf{B}} + \nabla \times (\underline{\mathbf{v}} \times \underline{\mathbf{B}})$$

- Reconnection occurs where/when **the resistive term** is high:
 - Possibly depends on local plasma condition: η can increase with temperature, depending on type of collisions, ...
 - Depends on the geometry of the magnetic field: the field must present strong rotational of the electric current density, i.e. **localized thin current sheet** $\mu_0 \mathbf{J} = \nabla \times \mathbf{B}$.
- Magnetic reconnection is a challenging process to understand because it couples strongly local and global scales

Active regions on the Sun:
the result of the interaction between
localized magnetic fields and the solar plasma



The activity phenomena in the solar atmosphere are due to the emergence of magnetic flux tubes and to their interaction with the ambient plasma.



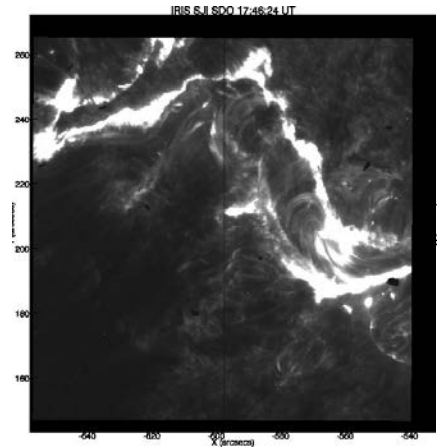
Given the physical conditions in the solar atmosphere, these phenomena can give rise to eruptive phenomena !

Back to solar eruptive phenomena

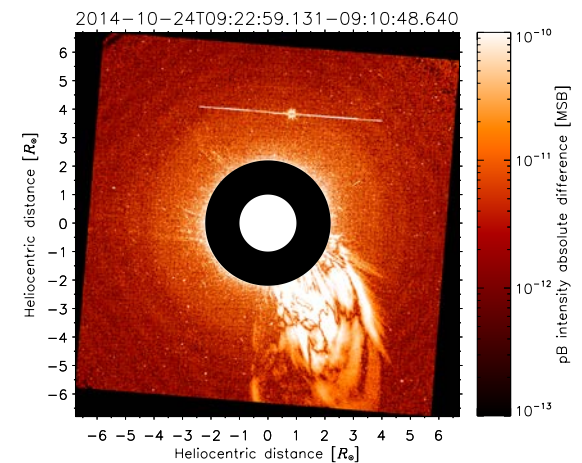
- *Filament eruptions*



- *Flares*



- *Coronal Mass Ejections*



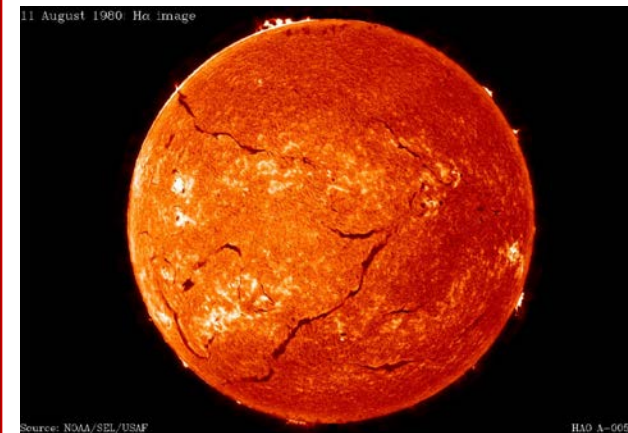
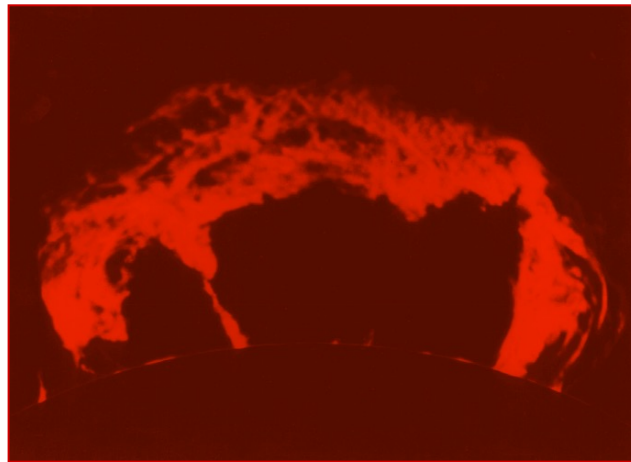
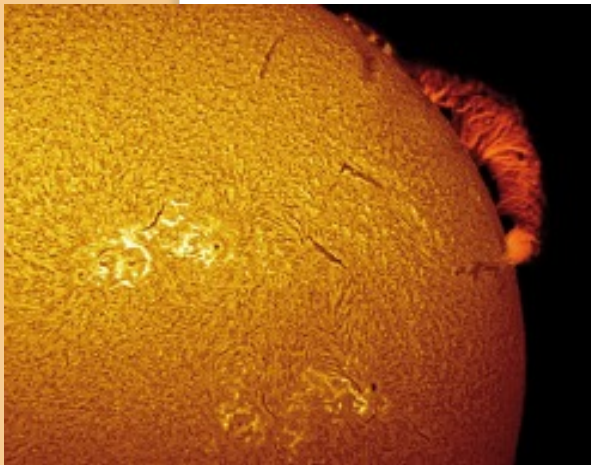
Filament / Prominences : classification

➤ Morphological classification (different size and dynamics)

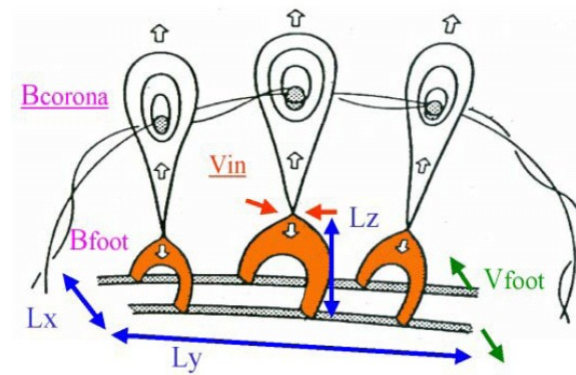
- ◆ **Active Region Prominences:** often characterized by sudden eruptions (associated to flares).
Short lifetimes (few hours or one-two days).
Located at low latitudes.
- ◆ **Quiescent Prominences:** very large size and often located at high solar latitudes.

↓ Size & Lifetime

↑ Magnetic field strength



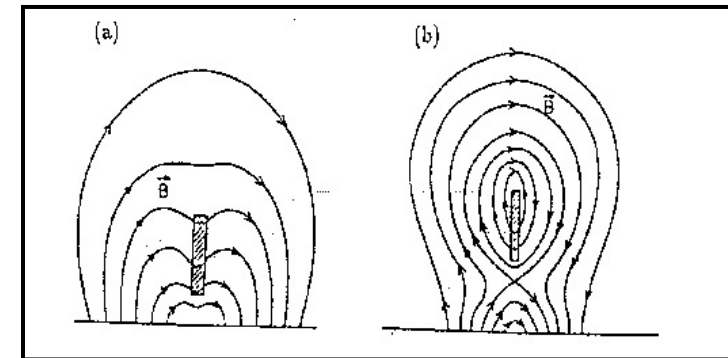
● Prominences are always located above a photospheric neutral (inversion) line that separates regions of opposite magnetic polarity;



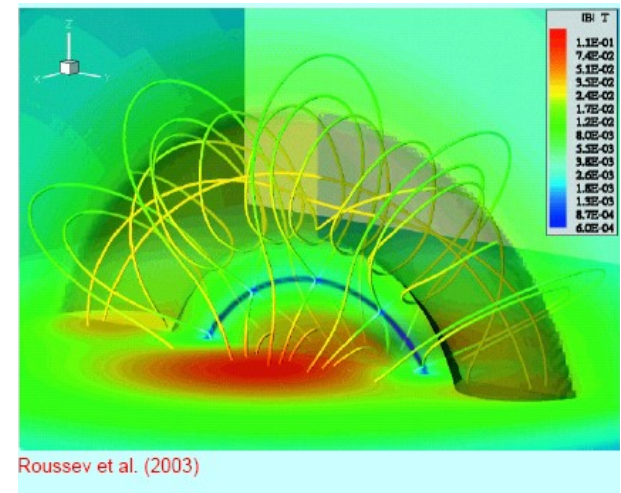
● Old observations and models: the magnetic field is mainly horizontal and can be characterized by a configuration called:



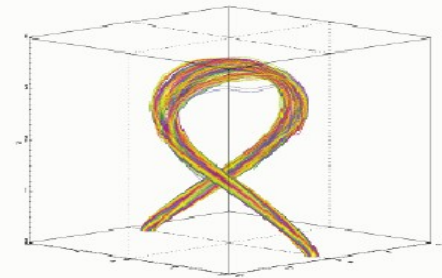
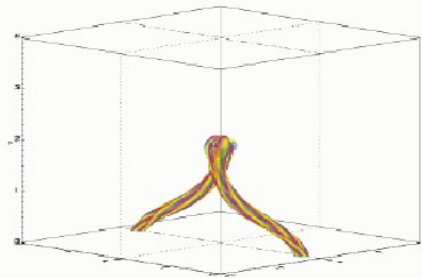
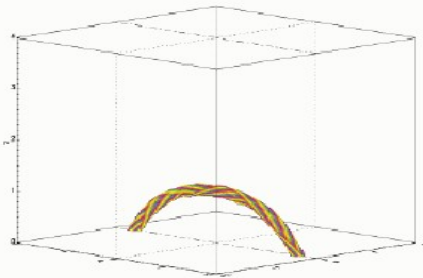
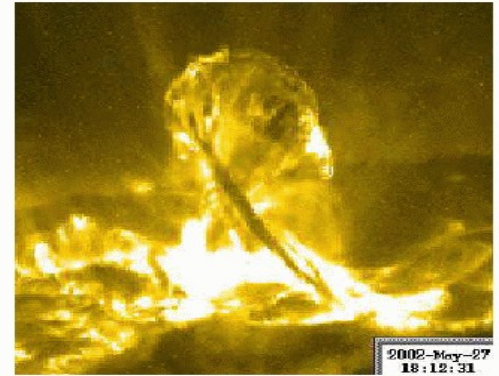
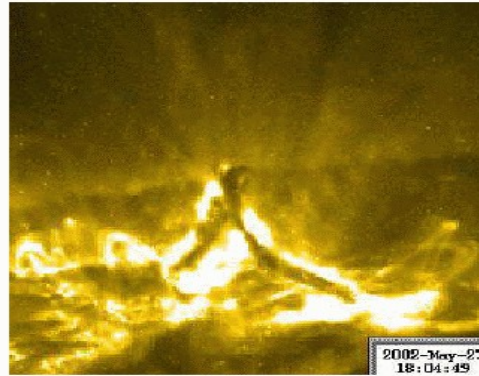
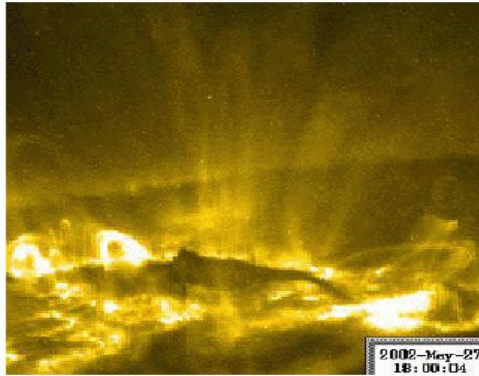
- (a) Normal: low latitudes and small size (~30000 Km)
- (b) Inverse: high latitudes and larger size



● New observations and models: Helical or twisted magnetic field configuration within the filaments (flux rope).



Filaments – Flux Ropes eruption

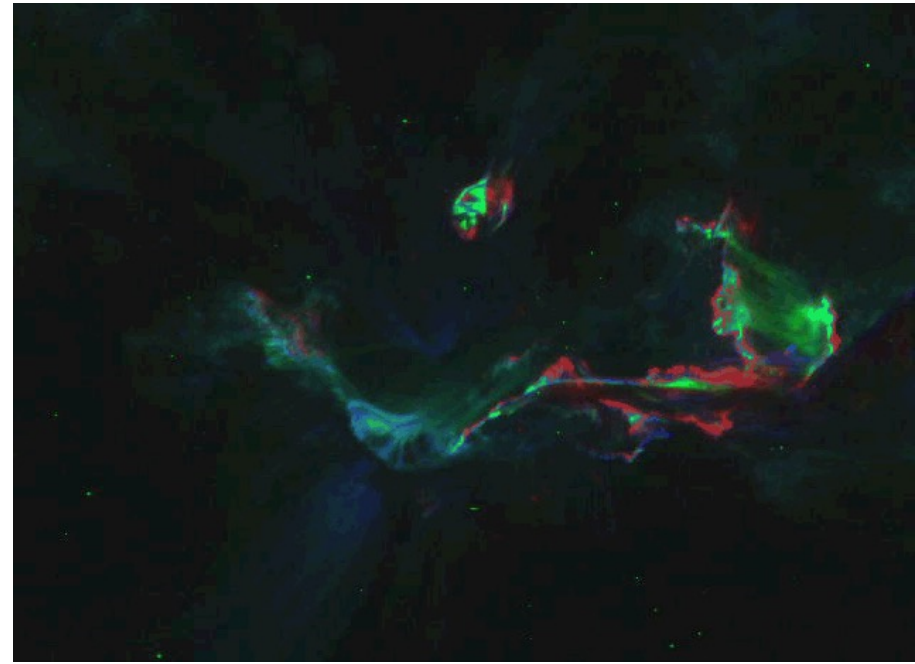


Top: TRACE 195 Å images of the confined filament eruption on 2002 May 27. The right image shows the filament after it has reached its maximum height. **Bottom:** magnetic field lines outlining the kink-unstable flux rope reproduced with 3D MHD simulations (Török & Kliem 2004).

SOLAR FLARES

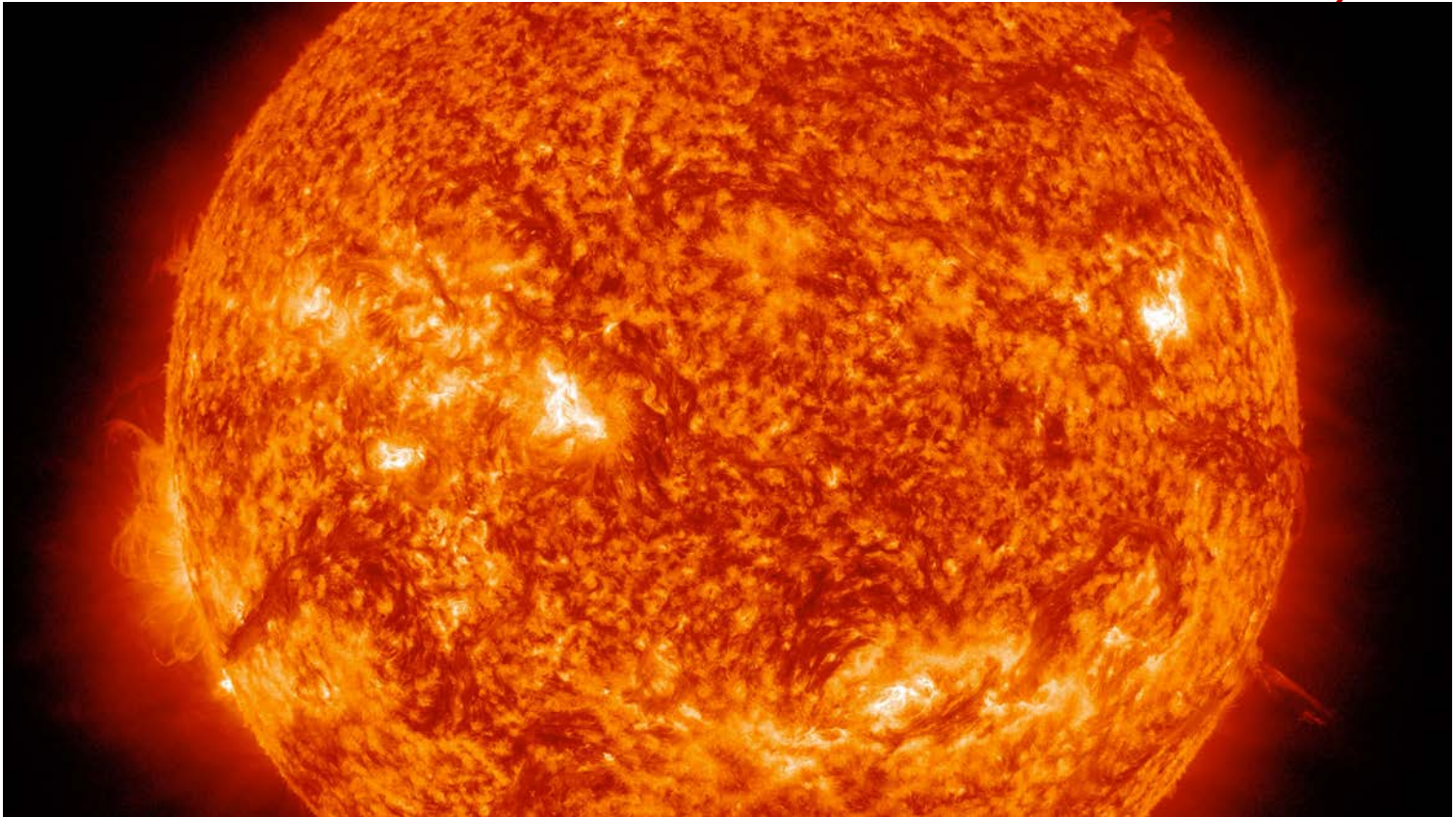
A solar flare is a sudden ($t_{\text{rise}} \sim$ few minutes), localized ($l \sim 10^6 - 10^8$ m), release of energy (from 10^{23} erg in nanoflares to 10^{32} erg in large two ribbon flares)

during which magnetic energy is converted into radiation across the entire electromagnetic spectrum, heating, particle acceleration and mass motions.



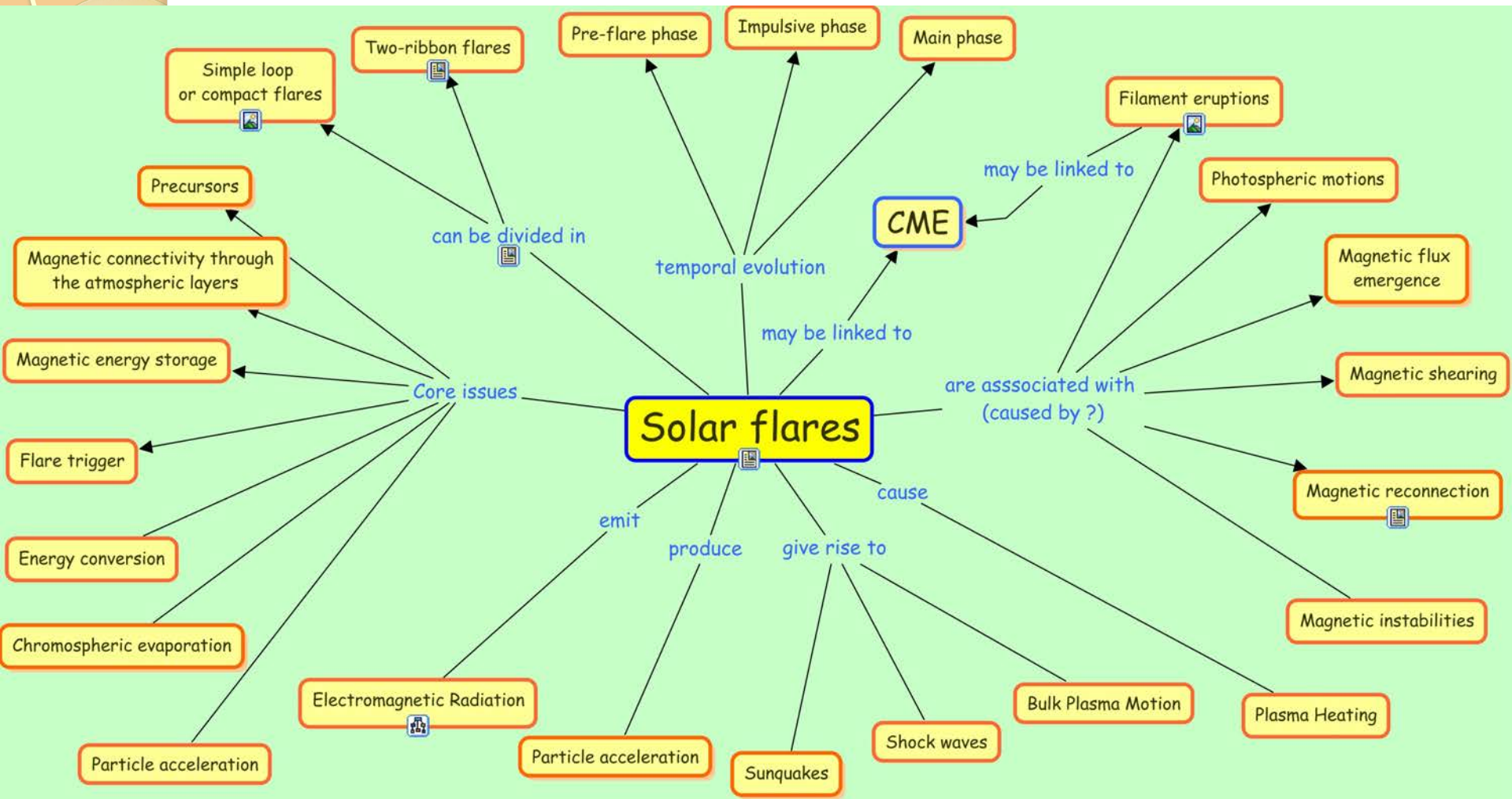
Class	Intensity ($\text{erg cm}^{-2} \text{s}^{-1}$)	I (W m^{-2})
A	10^{-5}	10^{-8}
B	10^{-4}	10^{-7}
C	10^{-3}	10^{-6}
M	10^{-2}	10^{-5}
X	10^{-1}	10^{-4}

Solar flares



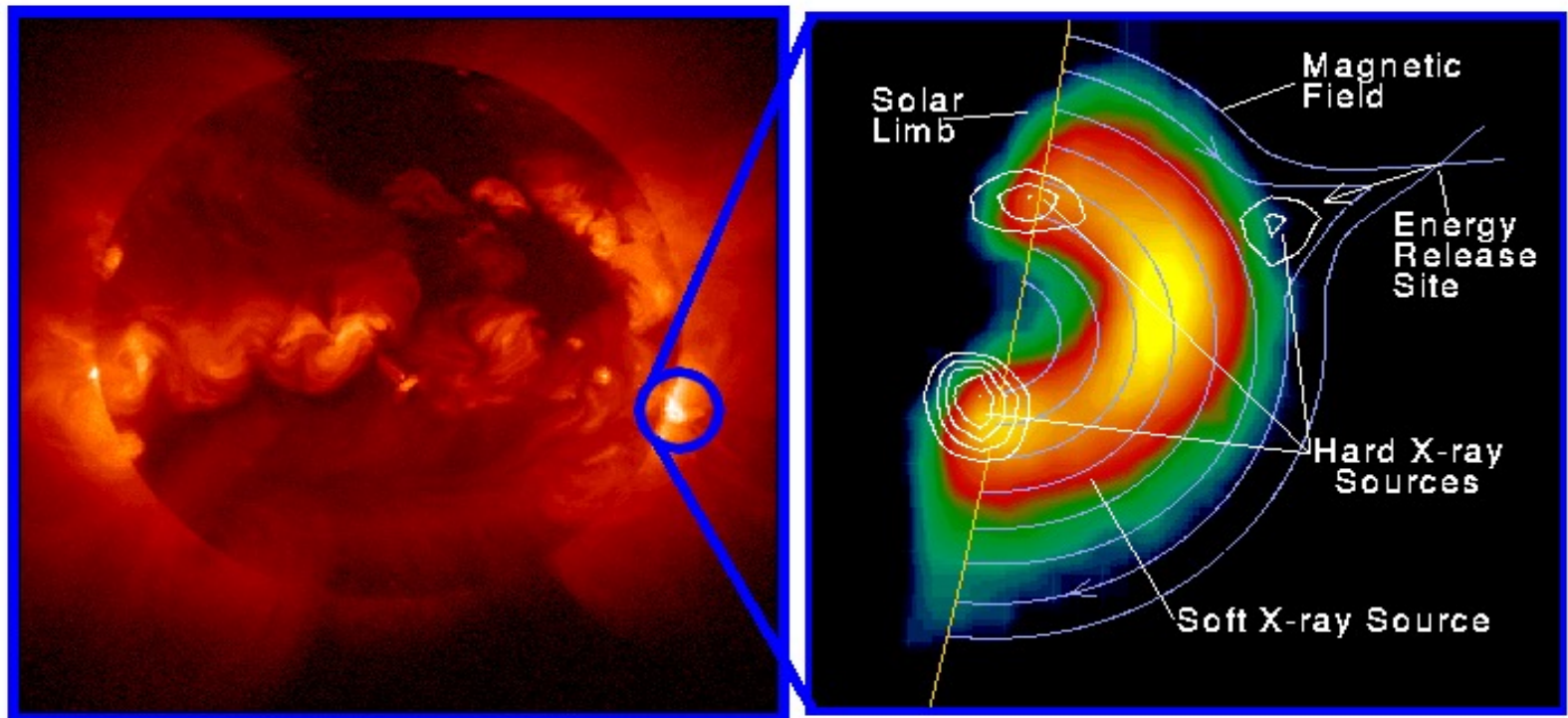
- *Solar flares can be (associated to) the most powerful events in the solar system*
- *Radiation and particles emitted during flares may strongly interact with Earth ionosphere and magnetosphere*
- *They represent an optimal tool to understand the physical processes involved in magnetic reconnection*

However, understanding solar flares is not an easy task!



Simple-loop flare

The HXR loop-top source indicates that energy release occurs high in the loop.



Yohkoh X-ray Image of a Solar Flare, Combined Image in Soft X-rays (left) and Soft X-rays with Hard X-ray Contours (right). Jan 13, 1992.

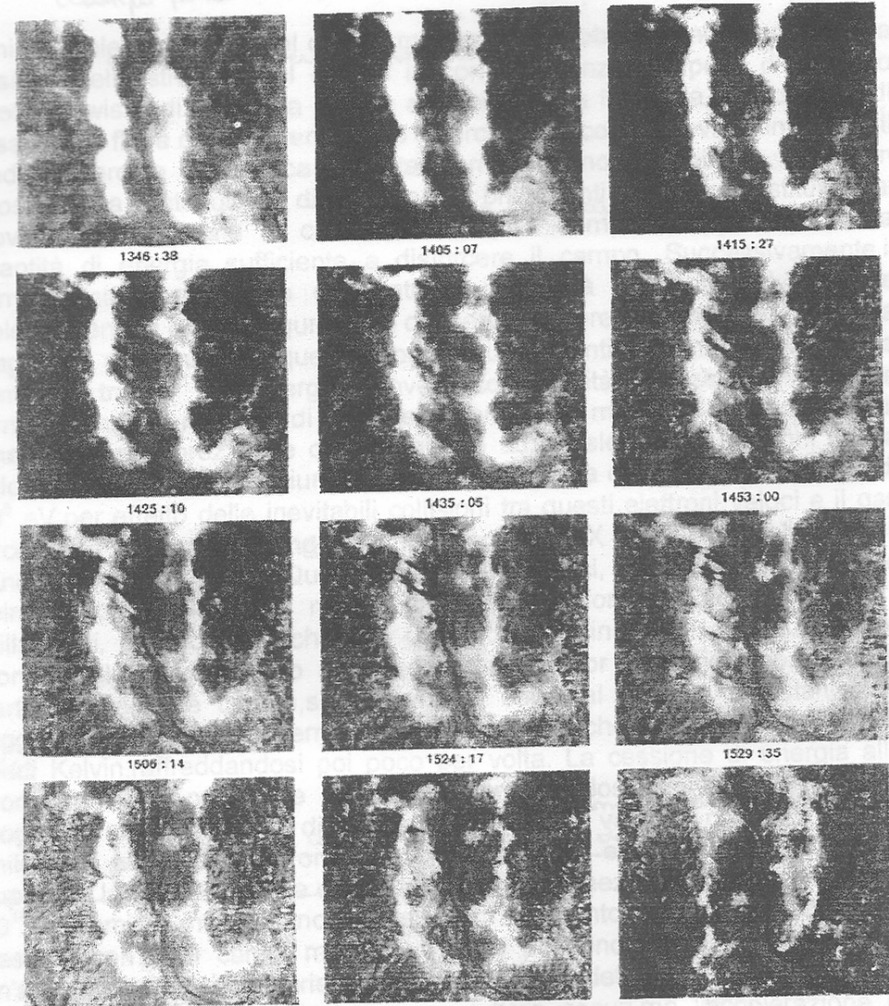
Two ribbon flares

- Historically, these events were firstly observed in the $H\alpha$ line

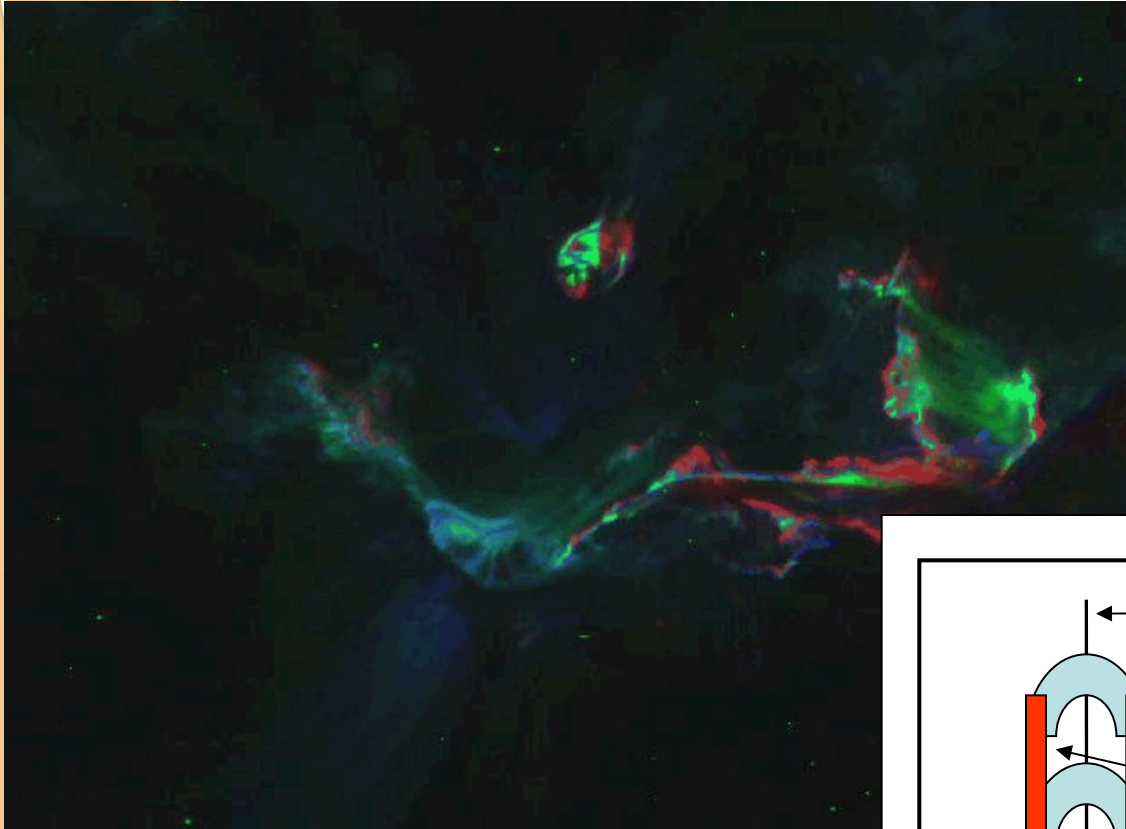
- Therefore they were classified as “chromospheric events”

- Two bright and parallel ribbons could be suddenly observed in the $H\alpha$ line

- The ribbons move apart as time goes on

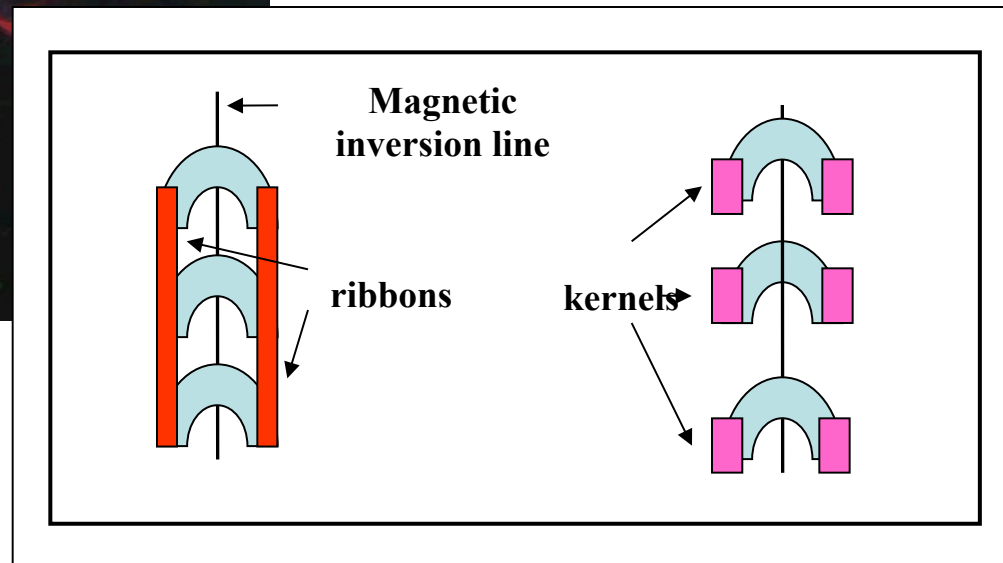


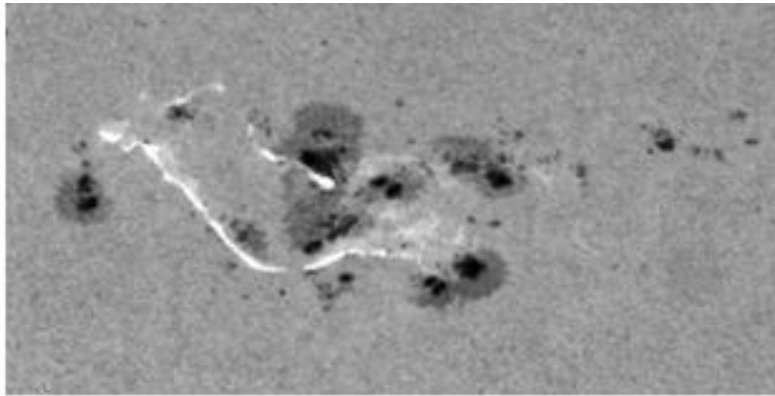
Change of perspective !!!!



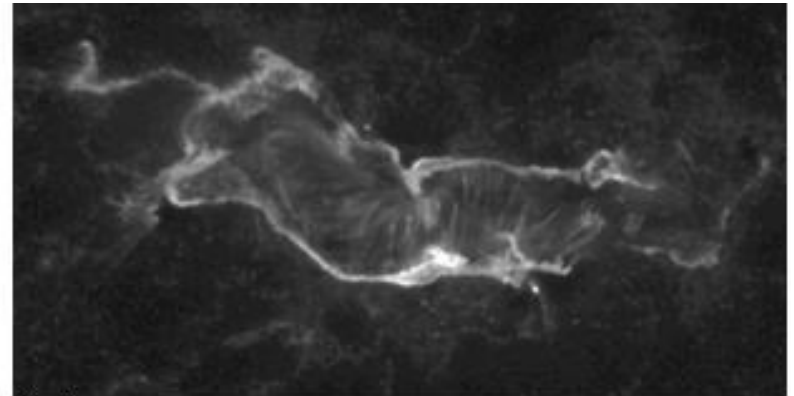
Bastille Day flare (14 July 2000).

(red: 1600 Å ; green: 171 Å and blue 195 Å).

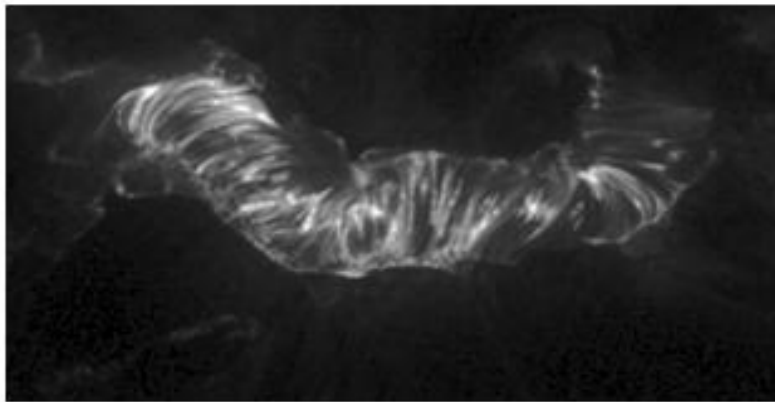




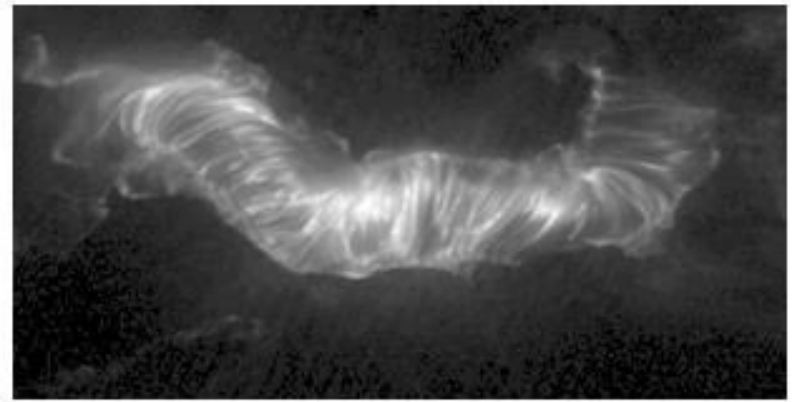
a)



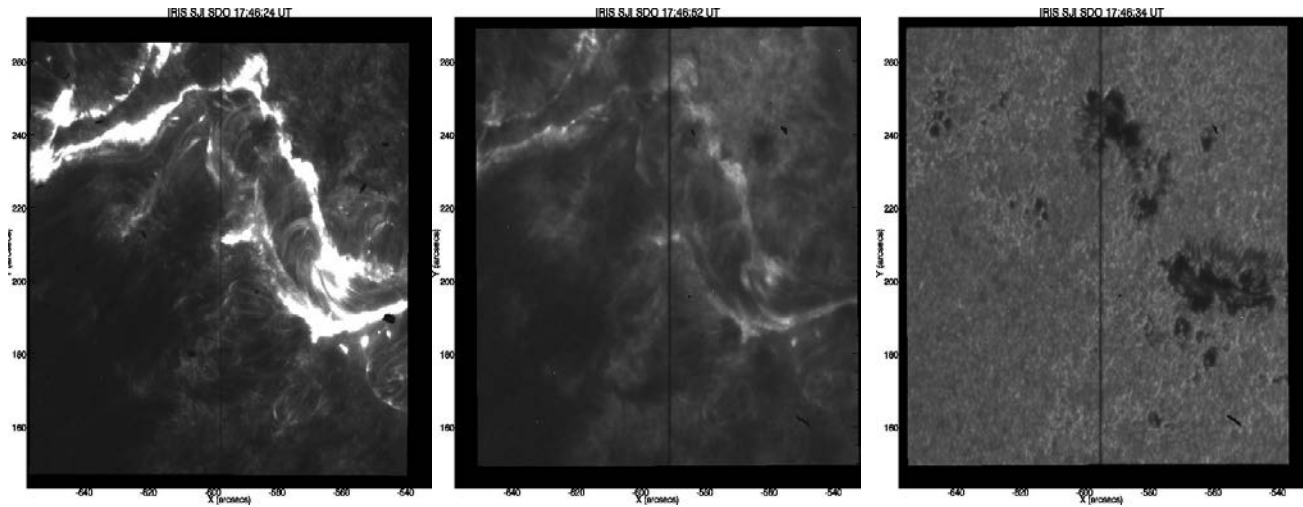
b)



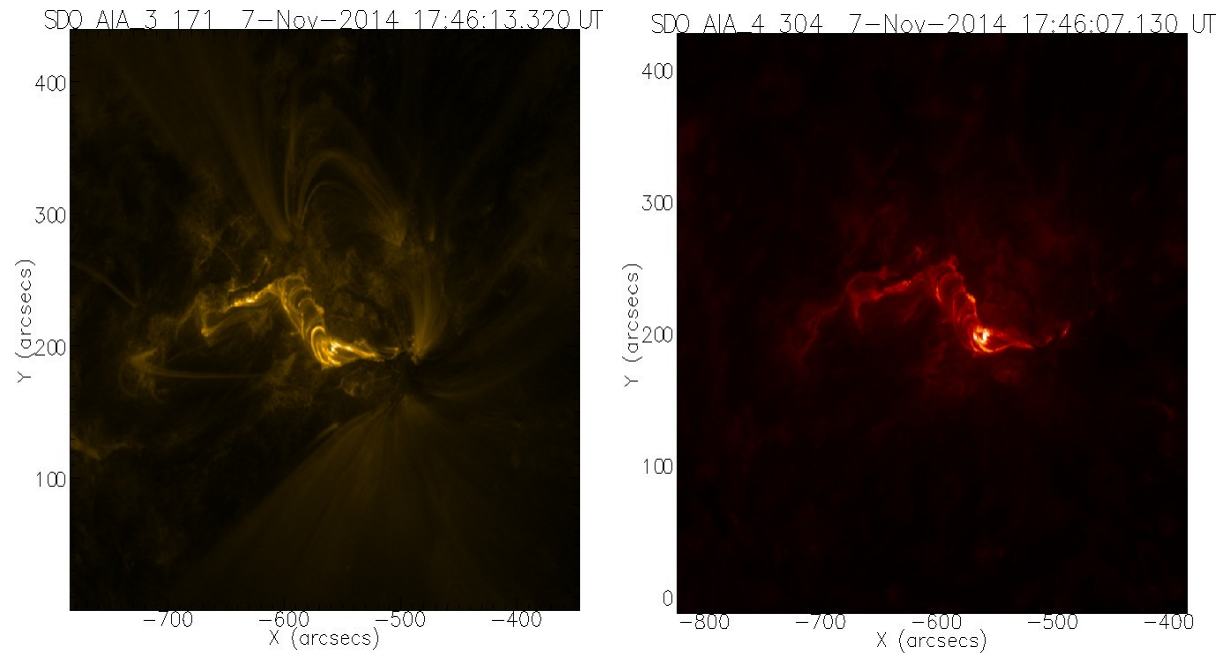
c)



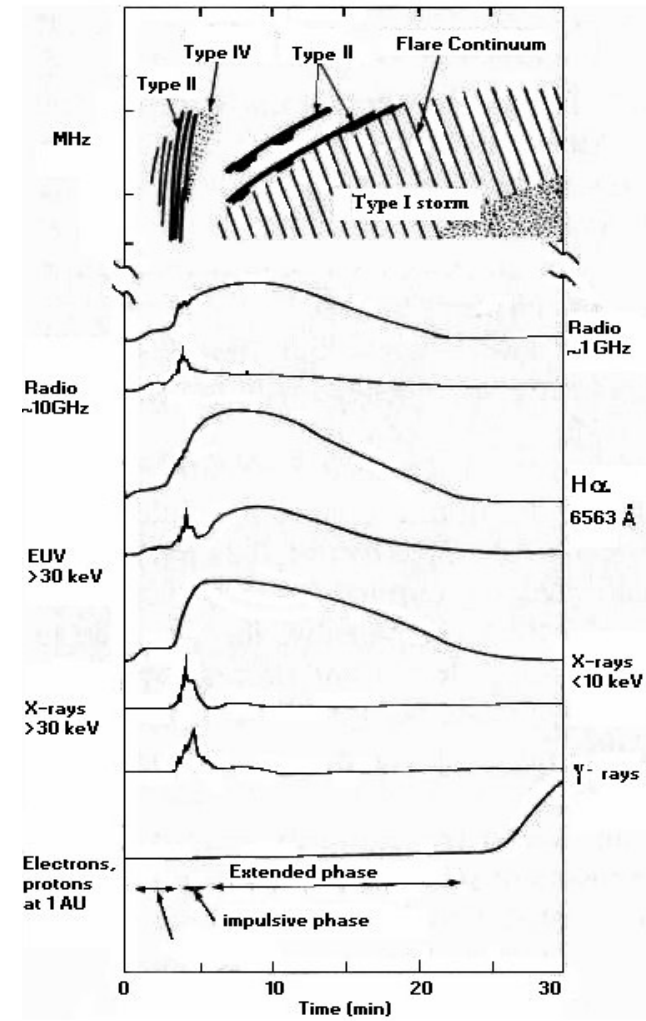
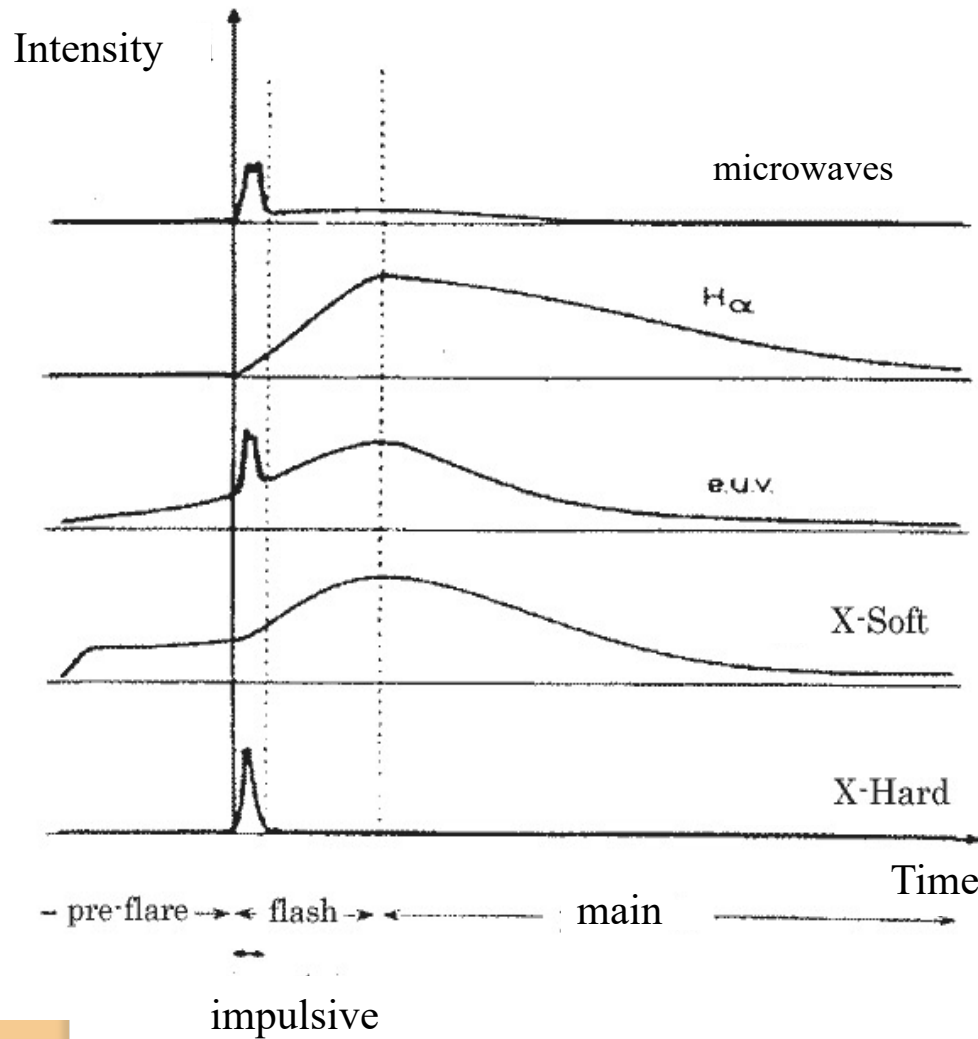
d)



A two ribbon flare observed by IRIS and SDO on 7 November 2015



Time profiles at different wavelengths

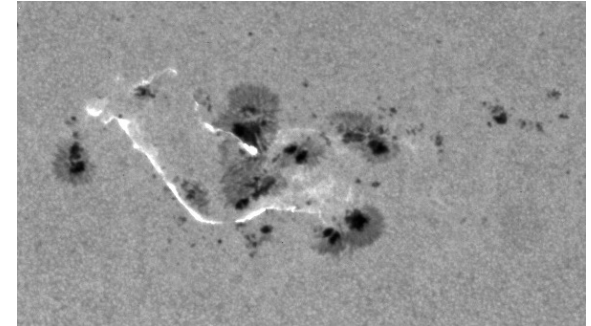


Observations at different λ

Optical range

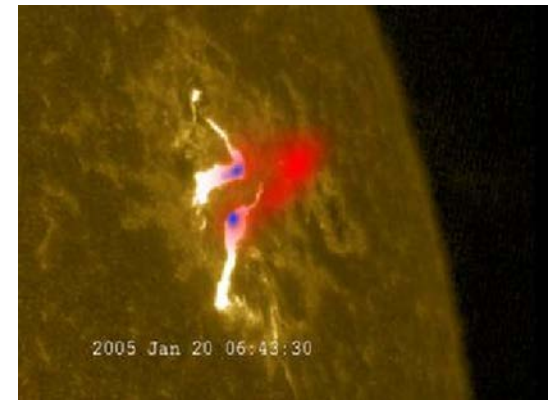
WL observations:

- morphology of the AR in photosphere
- signatures of WL ribbons (down to C2.0, Jess et al., 2008)



H α observations

- filament activation and rise
- H α ribbons or kernels
- post-flare H α loops
- comparison with models: changes of line profiles during flares

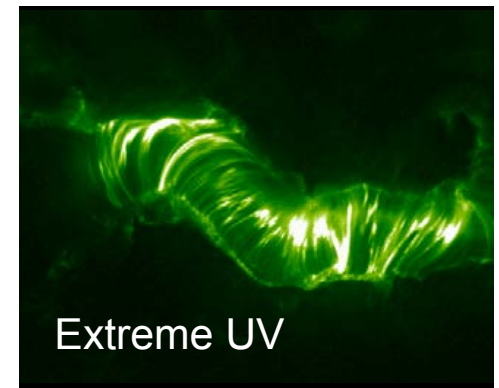
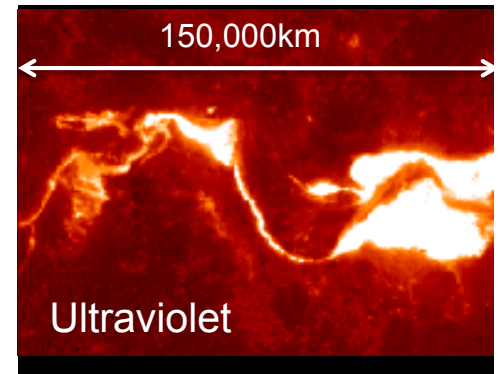


RHessi soft X-rays (red 8–12 keV) and HXR (blue 20–50 keV) overlaid on a H α image.

Observations at different λ

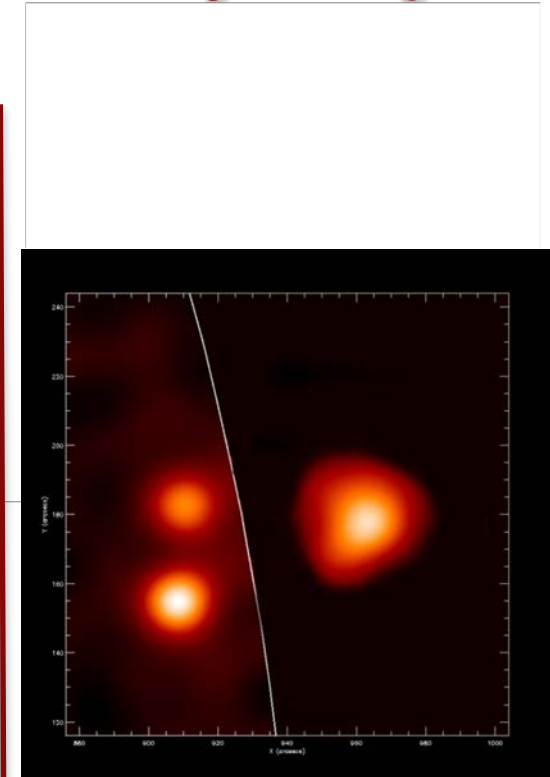
UV/EUV range

- Configuration of the AR in chromosphere - transition region - corona
- Plasma evaporation/condensation
- UV/EUV post-flare loops (timing, spatial configuration, correlation with WL/H α ribbons)
- Hints on the fine structure of erupting filaments - flux ropes
- Plasma diagnostics (temperature, density, emission measure)



Flare observations at different λ X-ray range

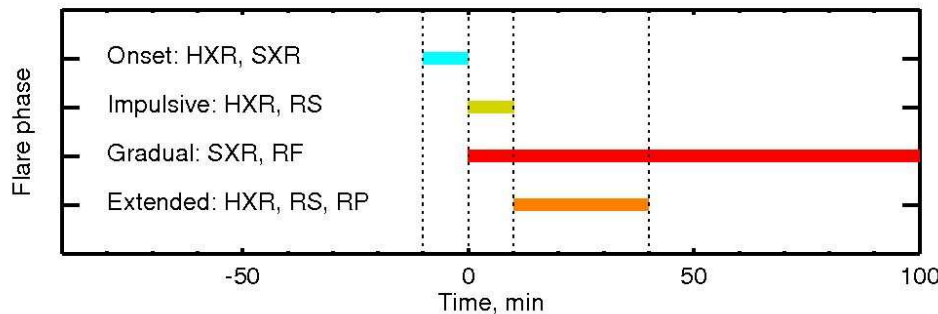
- **Soft X-rays:** impulsive brightening (due to thermal emission) in loops connecting ribbons, related to chromospheric evaporation.
- **Hard X-ray sources** - One source is located above the soft X-ray loops. The others, caused by bremsstrahlung of colliding electrons, appear at chromospheric heights, as expected in the thick-target model (Brown et al., 1983; Kane, 1983)
- **Hard X-ray quasi-periodic pulsations** (10 s or minutes) \rightarrow sausage mode altering B in the loop and trapped particles precipitation rates.
- **Hard X-ray spectrum:** non-thermal shape, close to a power-law. It is used as an input for models (i.e. Radyn, Flarix)



Flare observations at different λ

Radio range

- Accelerated particles precipitate spiraling along the magnetic field lines
- In the range 1 – 100 GHz radio emission results from gyration of mildly relativistic electrons in the magnetic field (gyrosynchrotron emission)



HXR (above ~ 20 keV), SXR ($T < \sim 30$ MK).

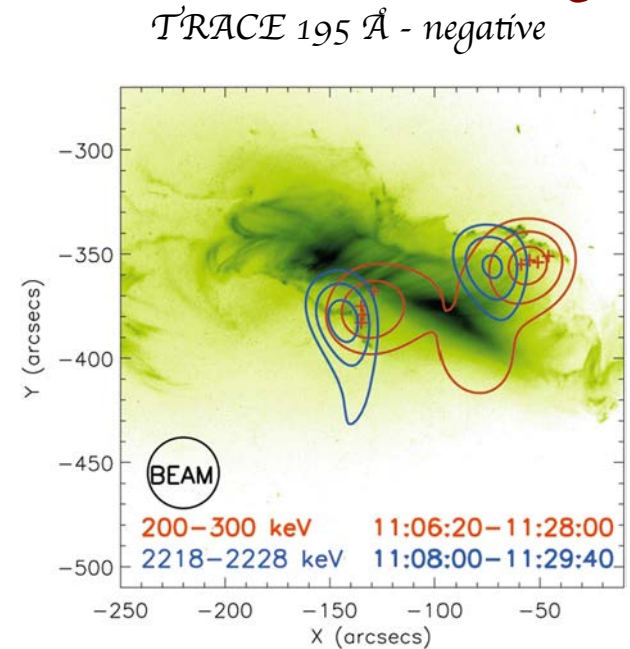
Radio emission is designated by RS (gyrosynchrotron), RF (free-free), RP (plasma-frequency mechanisms)

Time ranges associated with the different phases of a flare.

Flare observations at different λ

γ range

- γ -ray lines (0.8 - 20 MeV) emitted by atomic nuclei excited by impinging ions.
- Not all flares show gamma-ray lines (Vilmer et al. 2011).
- Most of the emission is confined to compact sources (Hurford et al., 2006).
- The footpoints of the 2.223 MeV line— indicating ion precipitation— and the footpoints of the non-thermal continuum emission—produced by precipitating electrons—do not always coincide.



Gamma-ray sources observed by RHESSI. In blue the deuterium recombination line at 2.223 MeV and in red the electron bremsstrahlung at 200-300 keV (Hurford et al., 2006).

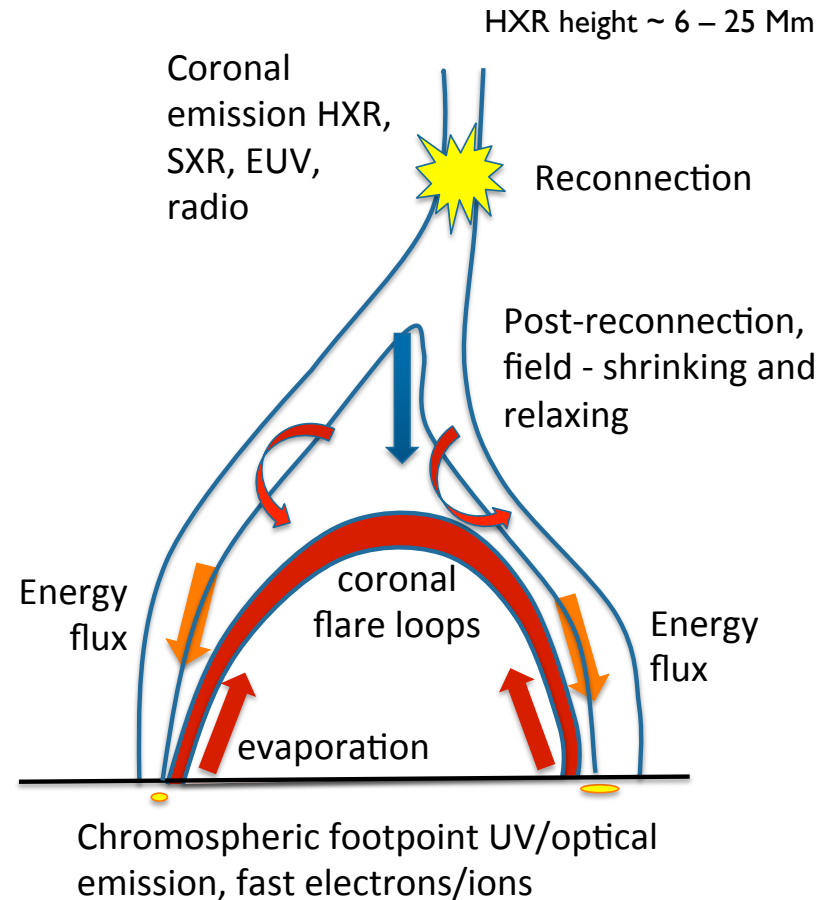
Flares:

Main Questions

The main question of flare physics is to understand:

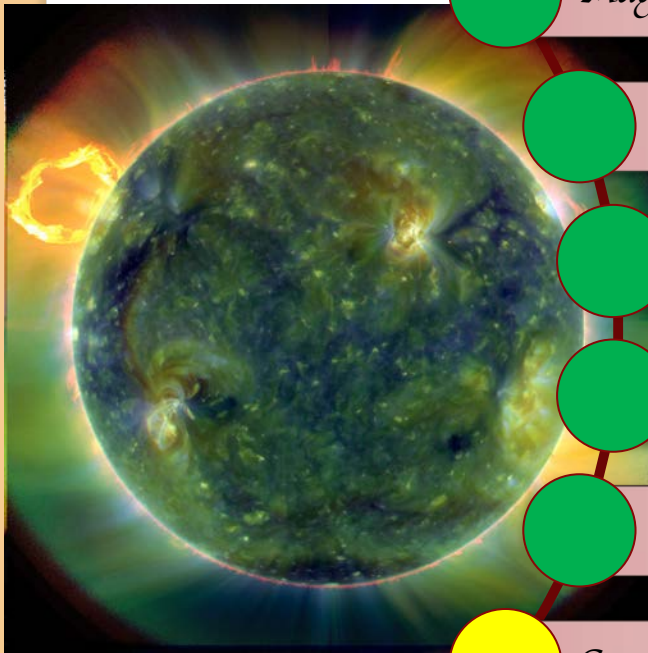
How the energy, previously stored in a stressed coronal magnetic field →







- *is released so rapidly,*
- *transported through the solar atmosphere,*
- *converted into the kinetic energy of the non-thermal particles and into the flare's radiation output.*



Fletcher, 2014

What is needed to produce an eruptive event (assuming you got the right star)



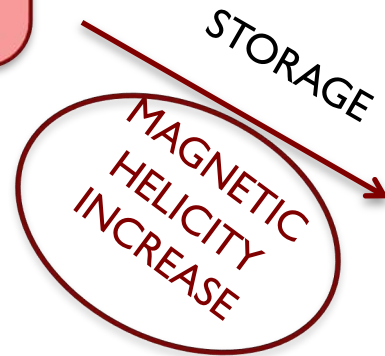
-  *Magnetic field*
-  *Stressed magnetic field (currents) - Magnetic energy storage*
-  *Trigger: Magnetic reconnection - Threshold - Instability*
-  *Energy conversion*
-  *Particle acceleration - e.m. emission - bulk plasma motions*
-  *Coronal mass ejection*

Magnetic energy storage

Potential
(current-free)
magnetic field

$$\nabla \times \vec{B} = 0$$

- Emergence of magnetic bundles (and frozen-in condition)
- Horizontal motions of the photospheric plasma at loop footpoints ($\sim 10^6 \text{ W m}^{-2}$)



Force-free
magnetic field

$$\nabla \times \vec{B} = \alpha \vec{B}$$

Electric currents
flowing parallel
to magnetic field
lines in corona

- ❖ Free magnetic energy: difference between the NLFF and a current-free field
- ❖ Some observations show that the free magnetic energy is stored only a few Mm above the photosphere
- ❖ The buildup of energy on its own does not guarantee the occurrence of an eruptive event (i.e., of a sudden energy release).

For a rapid release, the currents must be concentrated into small regions (Priest and Forbes, 2000)

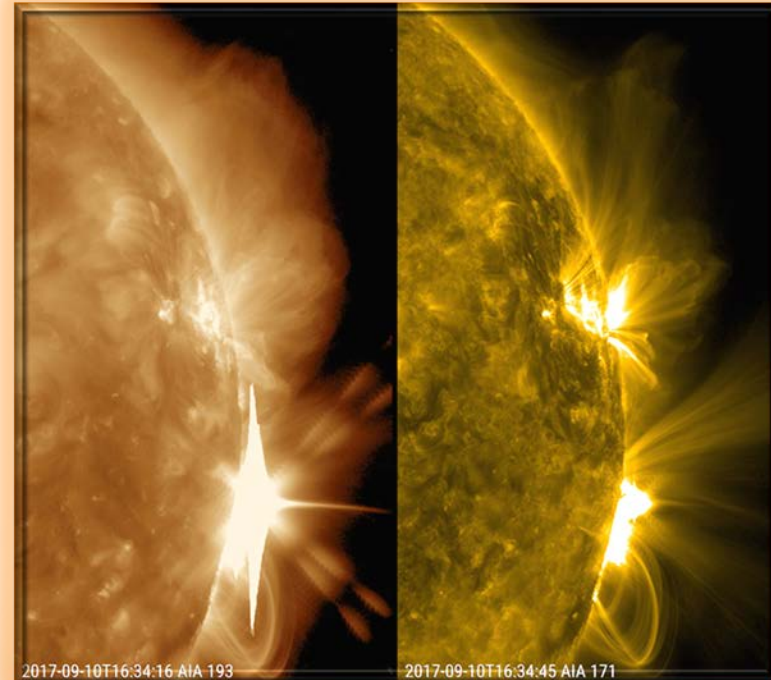


Current sheets
(magnetic field and plasma are
locally decoupled) →
reconnection

- $l \sim 100 - 1000 \text{ km}$
- $t \sim 1 \text{ s to } 10 \text{ min}$
- $h \sim 20 \text{ Mm}$ (from FF models of ARs)
- Not all the free energy is released

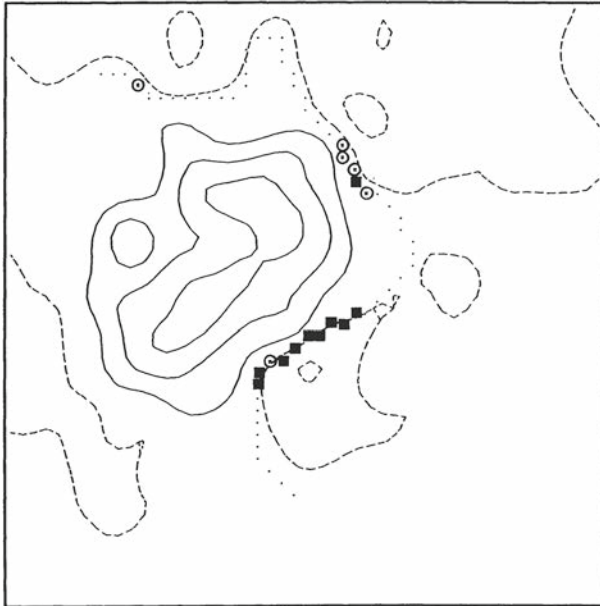
What triggers the eruption ?

- ❖ Magnetic reconnection
- ❖ Exceeding of a *threshold* (magnetic gradient, shear angle, height of the flux rope, accumulated magnetic helicity, ... magnetic field complexity - δ -spots)
- ❖ New *emergence* of magnetic flux within an already stressed magnetic field configuration
- ❖ Magnetic field *cancellation*
- ❖ Instabilities due to *nearby eruptions*



Shear angle

Magnetic field map
(MSFC magnetograph).



16:42 UT FEBRUARY 3, 1986

Solid: positive field
Dashed: negative field
Dotted: neutral line.

Circles : the transverse field deviates between 70° and 80° from the potential field (perpendicular to the neutral line).

Filled squares : deviations $>80^\circ$.

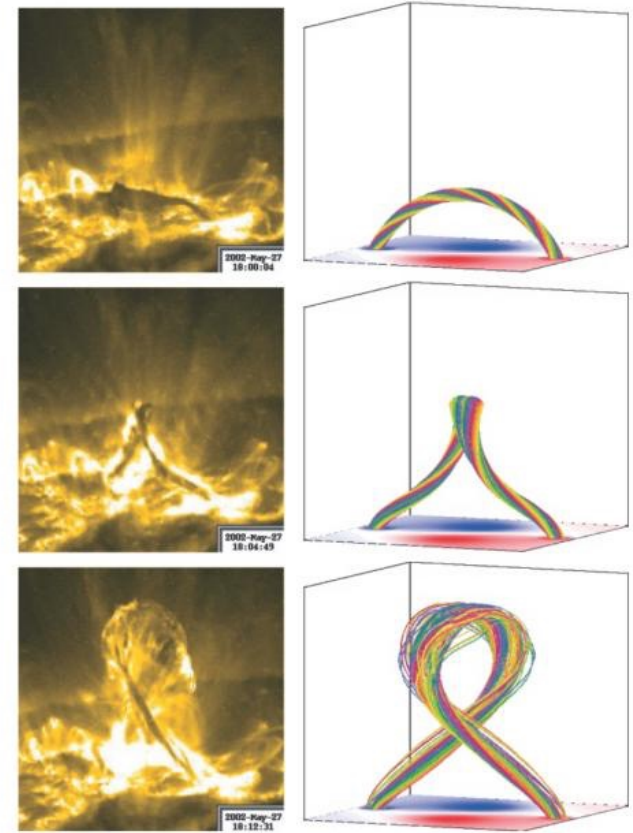
A large flare (X₃ class) occurred several hours later at the location of the largest shear.

Hagyard et al. (1990)

Kink instability

A flux tube twisted beyond a certain critical limit becomes unstable and kinks.

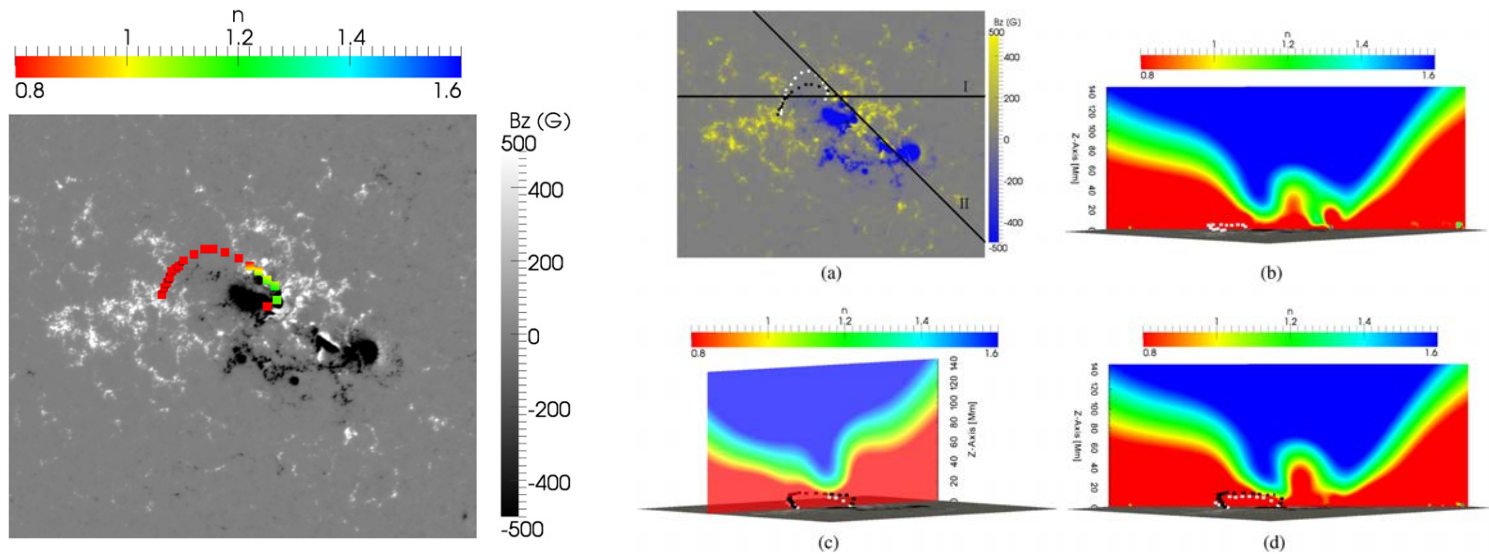
For a **twist** between 2.5π and 2.75π the system undergoes a rapid expansion - no stable equilibria exist anymore (Török & Kliem, 2003).



The Astrophysical Journal Sept. 2005 © American Astronomical Soc.

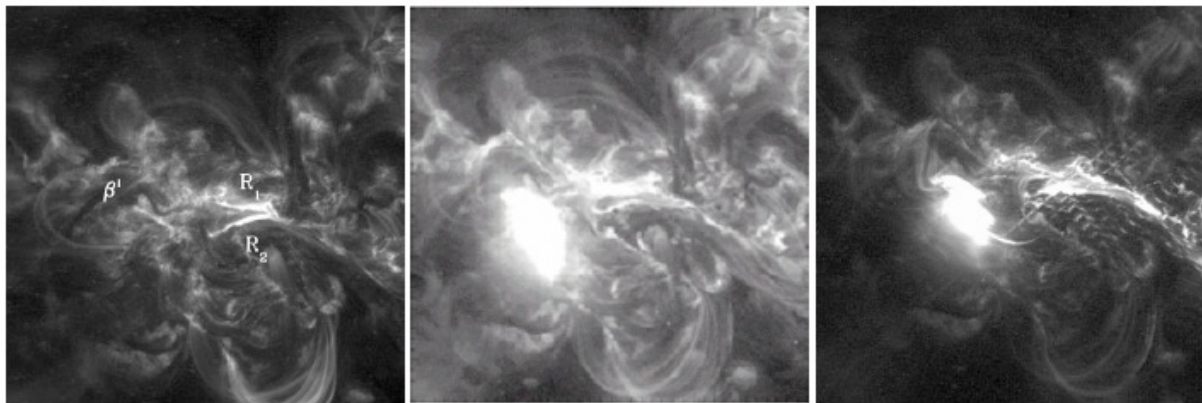
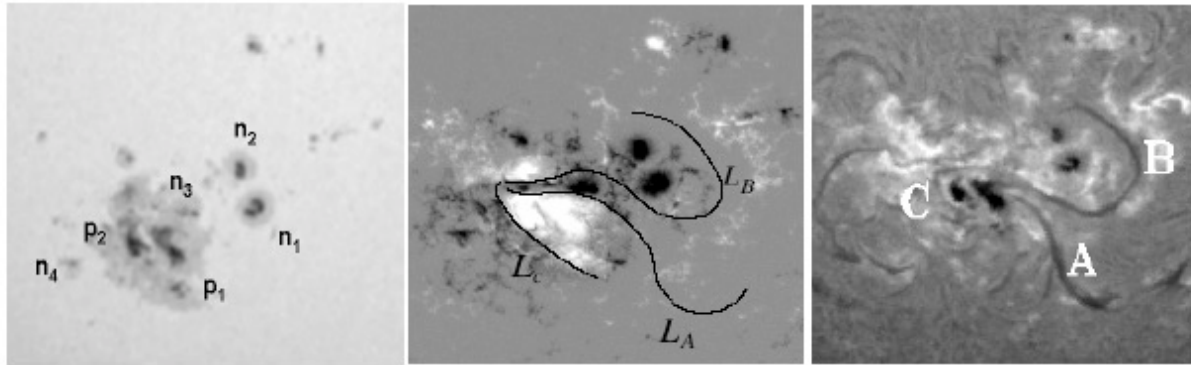
FIG. 1.—*Left:* TRACE 195 Å images of the confined filament eruption on 2002 May 27. *Right:* Magnetic field lines outlining the core of the kink-unstable flux rope (with start points in the bottom plane at circles of radius $b/3$) at $t = 0, 24,$ and 37 . The central part of the box (a volume of size 4^3) is shown, and the magnetogram, $B_z(x, y, 0, t)$, is included.

Torus instability

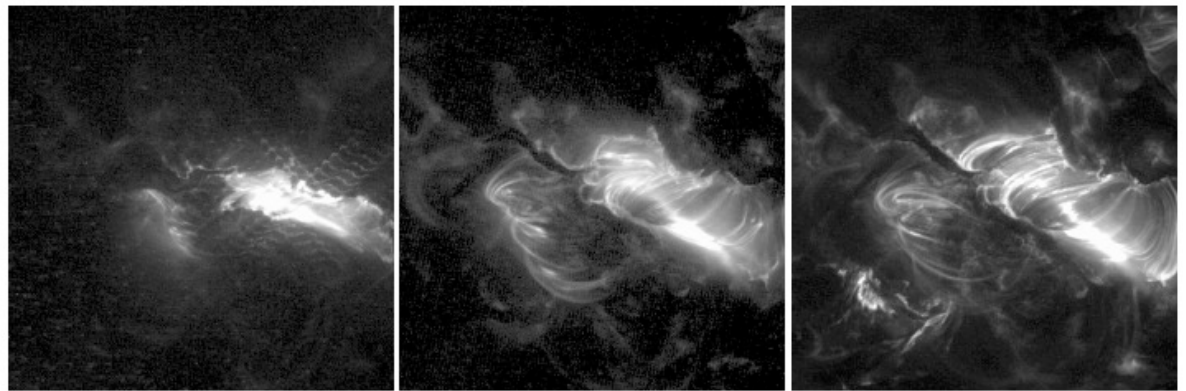


- ✓ When a flux rope reaches the altitude where the *decay index* for the magnetic field is $\sim 3/2$ (via photospheric flux-cancellation and tether-cutting coronal reconnection), it undergoes a rapid upward acceleration (Aulanier et al., 2010).

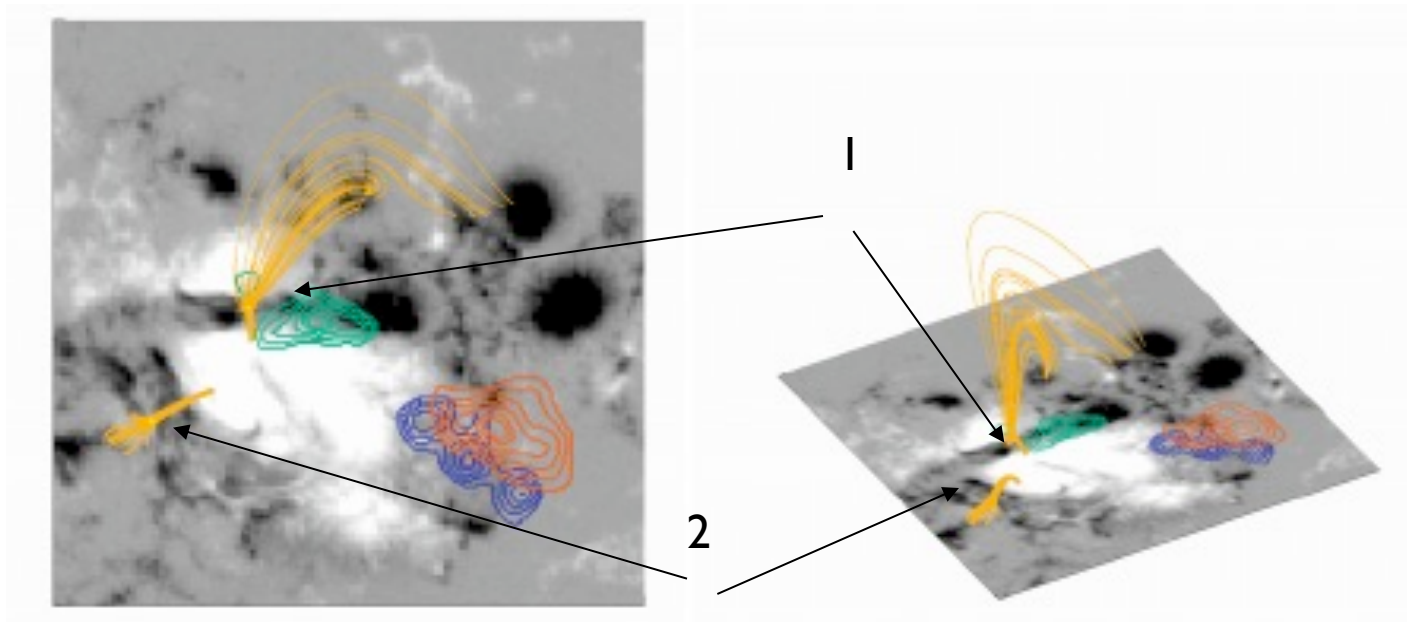
An X17.2 flare caused by a *domino* effect



The peak of the X17.2 flare was registered by GOES ~ 2 hr later than the first filament eruption



Null points and hard X-ray sources

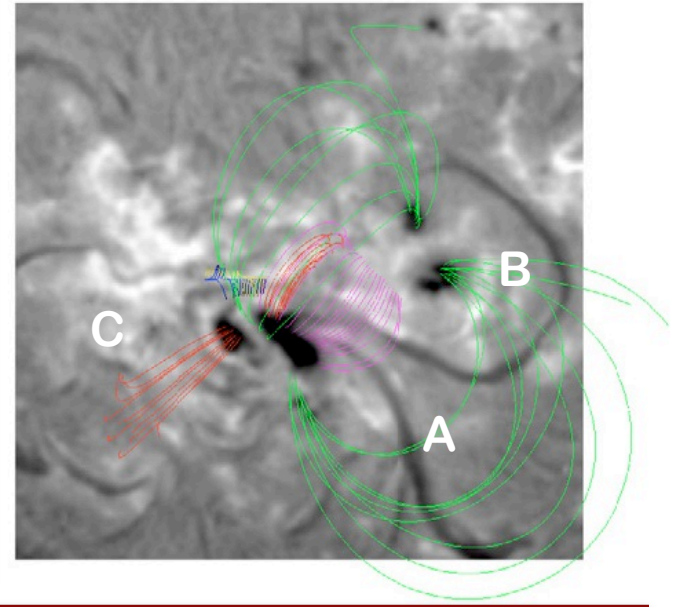


Magnetic field lines and null points overplotted on the MDI magnetogram: the null point 1 is located in the proximity of a negative intrusion, while the null point 2 is located on the eastern side of filament C.

The images show also the hard X-ray sources at 07:55:42 UT (blue), 08:16:30 UT (green), and 11:22:08 UT (red-brown).

Null points or QSL are sites where magnetic reconnection is triggered.

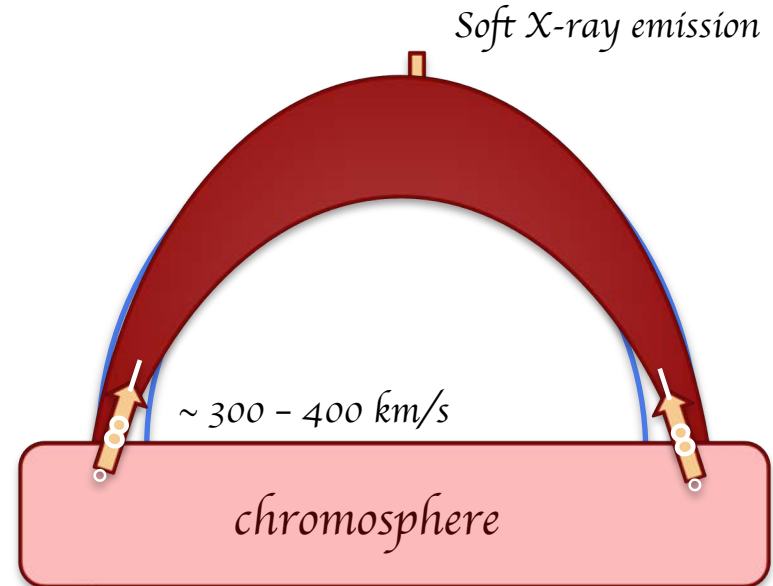
- 1) Multipolar magnetic field configuration.
- 2) Activation and/or eruption of three filaments.
- 3) Brightenings during the preflare and impulsive phases in sites corresponding to separatrix surfaces;
- 4) Post-flare loops observed almost simultaneously in distant arcades.



Interpretation: successive destabilizations of the magnetic field configuration, by a *domino effect*: filament A eruption → lift-off of the inner (magenta) arcade → reconnection at null points located in the lower atmosphere → decrease of tension in the higher (green) arcade → destabilization of filaments B and C → X17.2 flare.

How eruptions affect the chromosphere: Chromospheric evaporation

- When energetic electrons and ions precipitate from the coronal acceleration site and impact on the dense chromosphere losing their energy via Coulomb collisions, the plasma responds dynamically
- The **temperature** in the chromosphere **increases** and the resulting pressure exceeds the ambient chromospheric pressure.
- If the overpressure builds up **sufficiently fast**, the heated plasma **expands explosively** along the magnetic field in both directions

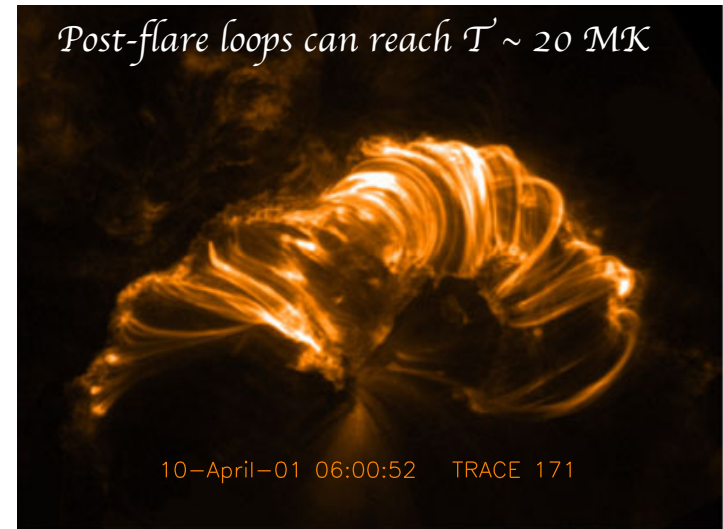


Gentle evaporation: $v \sim 65 \text{ km/s}$,
probably driven by a non-thermal
electron flux $< 3 \times 10^{10} \text{ erg cm}^{-2} \text{ s}^{-1}$

Chromospheric evaporation

- SXR and EUV post-flare loops form and grow, filled by chromospheric plasma
- The SXR plasma is not heated by the primary flare energy release, but is a secondary product when flare energy is transported to the chromosphere.
- Different scenario proposed by Fletcher & Hudson (2008): energy transported by Alfvén waves.

Fletcher et al., Space Sci. Rev. 2011

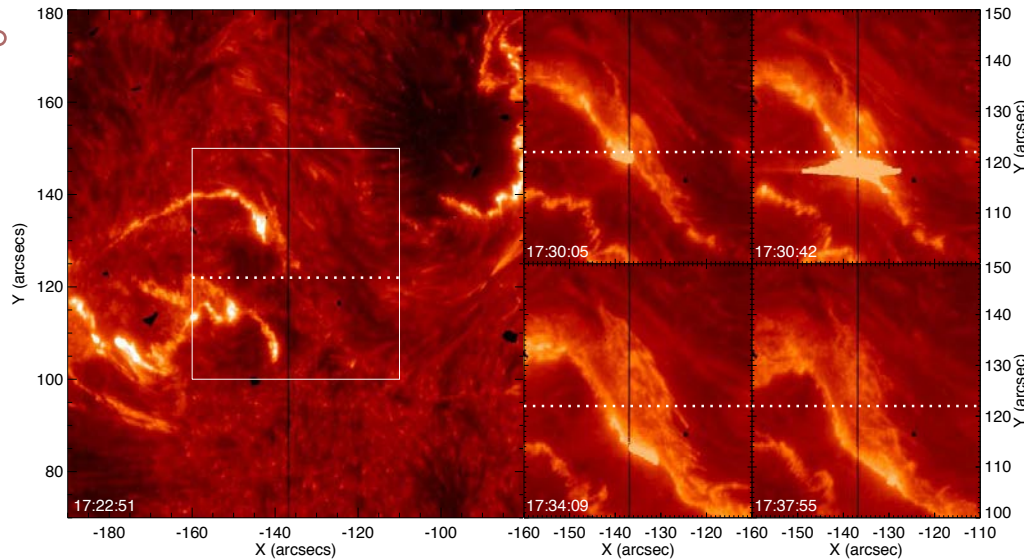


Later on, the arcade becomes visible in lower temperature emissions, including H α (Schmieder et al. 1995) .

Cooling occurs by both 1) conduction and 2) radiation.

The cool loop plasma drains under gravity, and H α downflows (“coronal rain”) become visible along the legs of the arcade.

Chromospheric evaporation / condensation in flaring loops

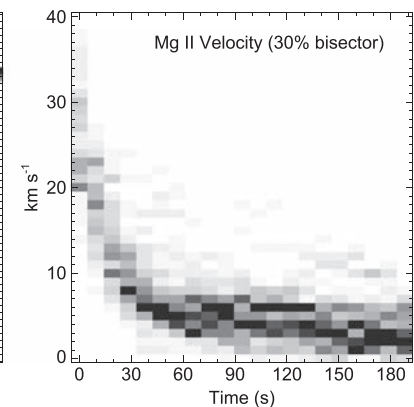
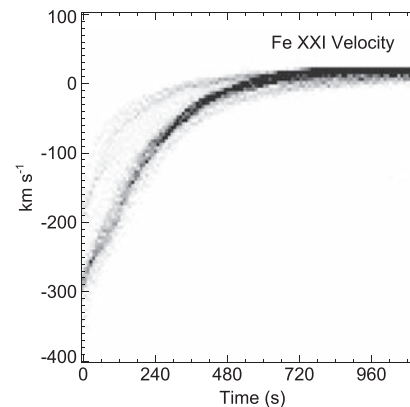


SOL20140910 (IRIS, SDO)

- X1.6 flare in NOAA 12158
- One ribbon moves down spectrometer slit (Fe XX1 - 10 MK)
- Velocity profiles obtained at 80 pixels along the IRIS slit

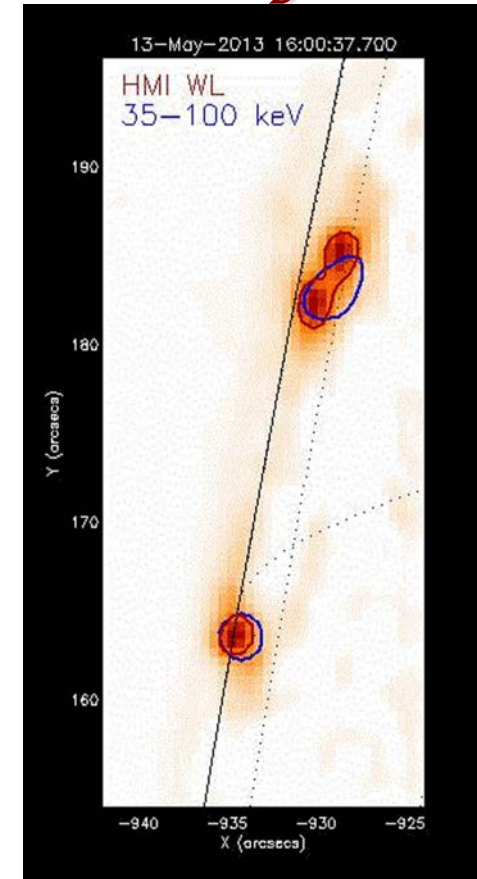
IRIS flow velocity as a function of time after first detection of flow for both ~ 20 MK (LH) and cool (RH) chromospheric plasma.

Each footpoint shows the same initial upflow of 300 km/s and chromospheric downflow of 40 km/s.



How eruptions affect the photosphere: WL flares

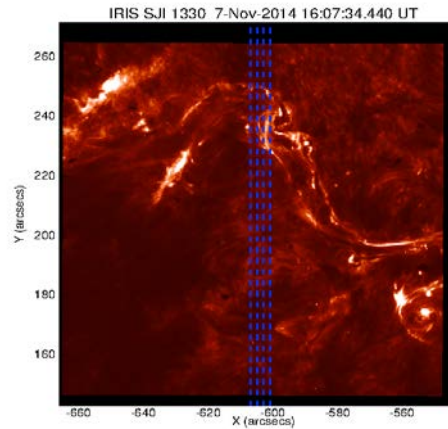
- ❖ WL flare emission correlate in time with hard X-rays (Matthews et al. 2003; Metcalf et al. 2003; Hudson et al. 2006).
- ❖ It also coincides in space within less than an arcsecond (Krucker et al. 2011).
- ❖ The source region of the WL emission is in the low chromosphere (Krucker et al. 2011; Martinez Oliveros et al. 2012).



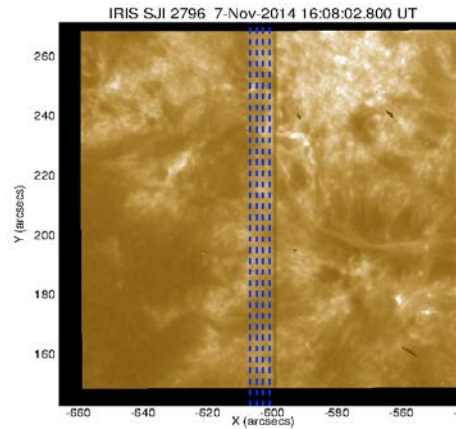
WL flare near the solar limb.
RHESSI HXR (30-50 keV,
blue) contours are overlaid on a
WL difference image
(HMI/SDO).

Observing Campaign “Searching for signatures of VWL flares”

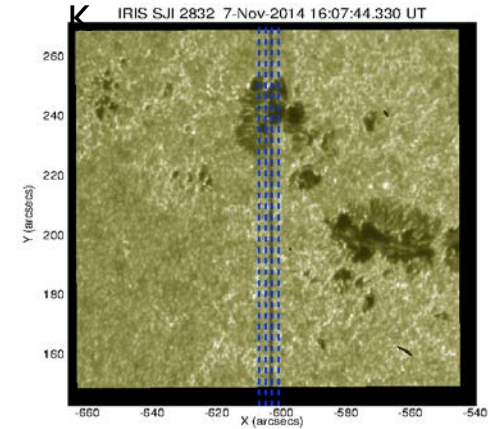
C II 1330 Å 30000 K



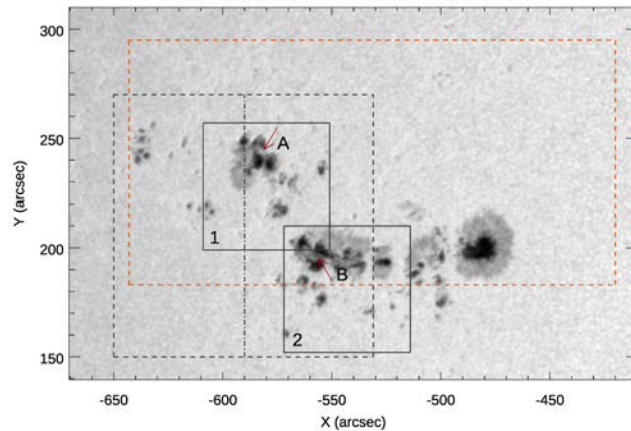
Mg II k 2796 Å 10000 K



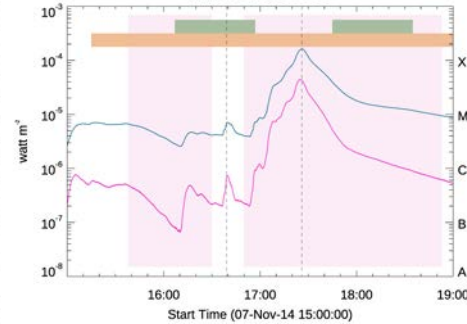
Mg II k wing 2832 Å 6000 K



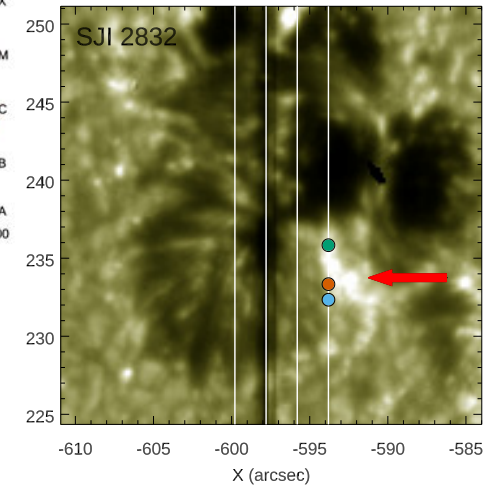
SDO/HMI Continuum 7-Nov-2014 16:58:12.9 UT



Flux GOES15 2 sec



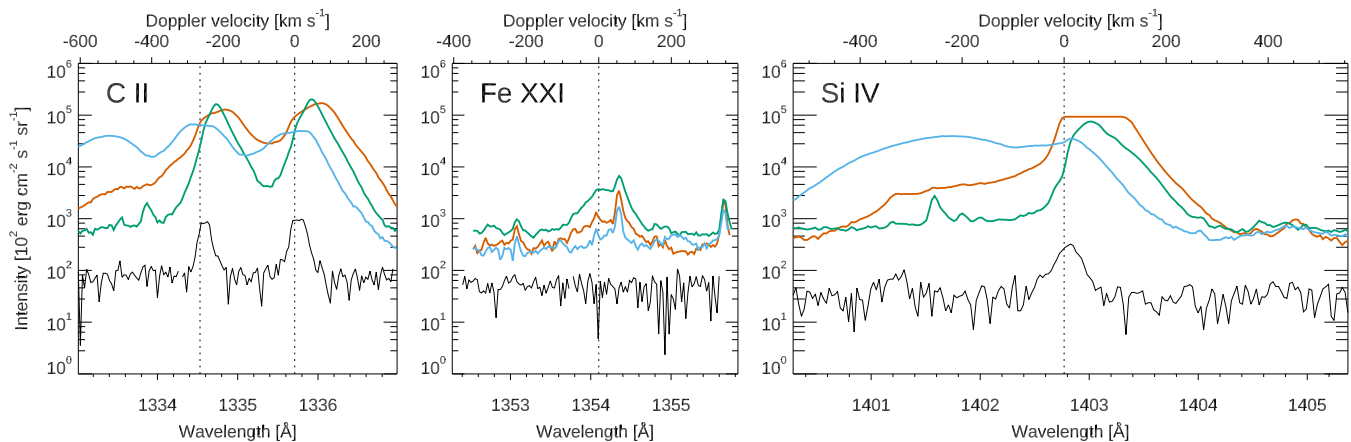
XI.6 flare



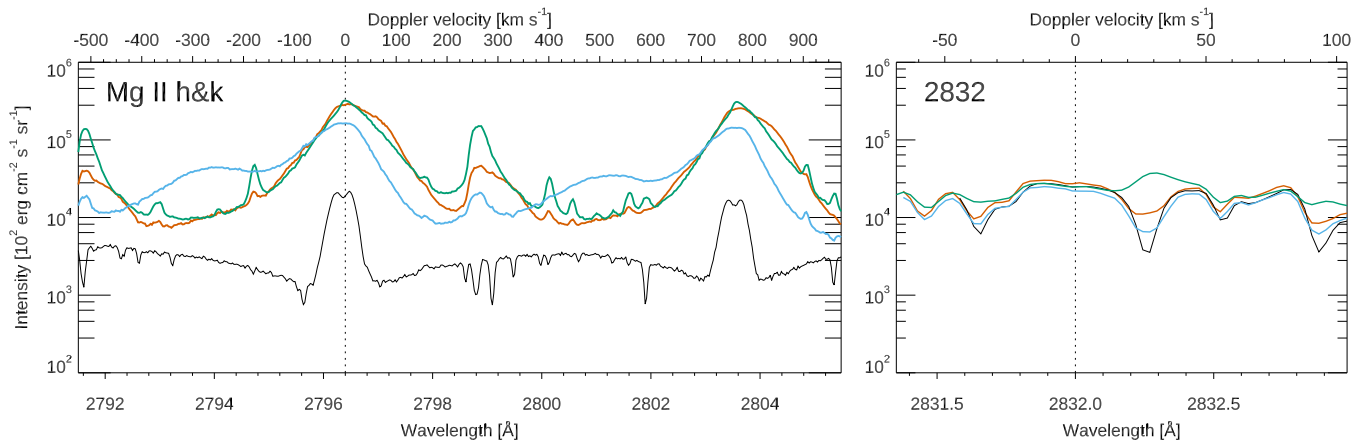
Zoomed IRIS 2832 Å slit-jaw image, showing the approximate location of the slits and three pixels analyzed in the following. The red arrow indicates a brightening.

Continuum enhancements in FUV and NUV @ the rise phase of the XI.6 flare

FUV

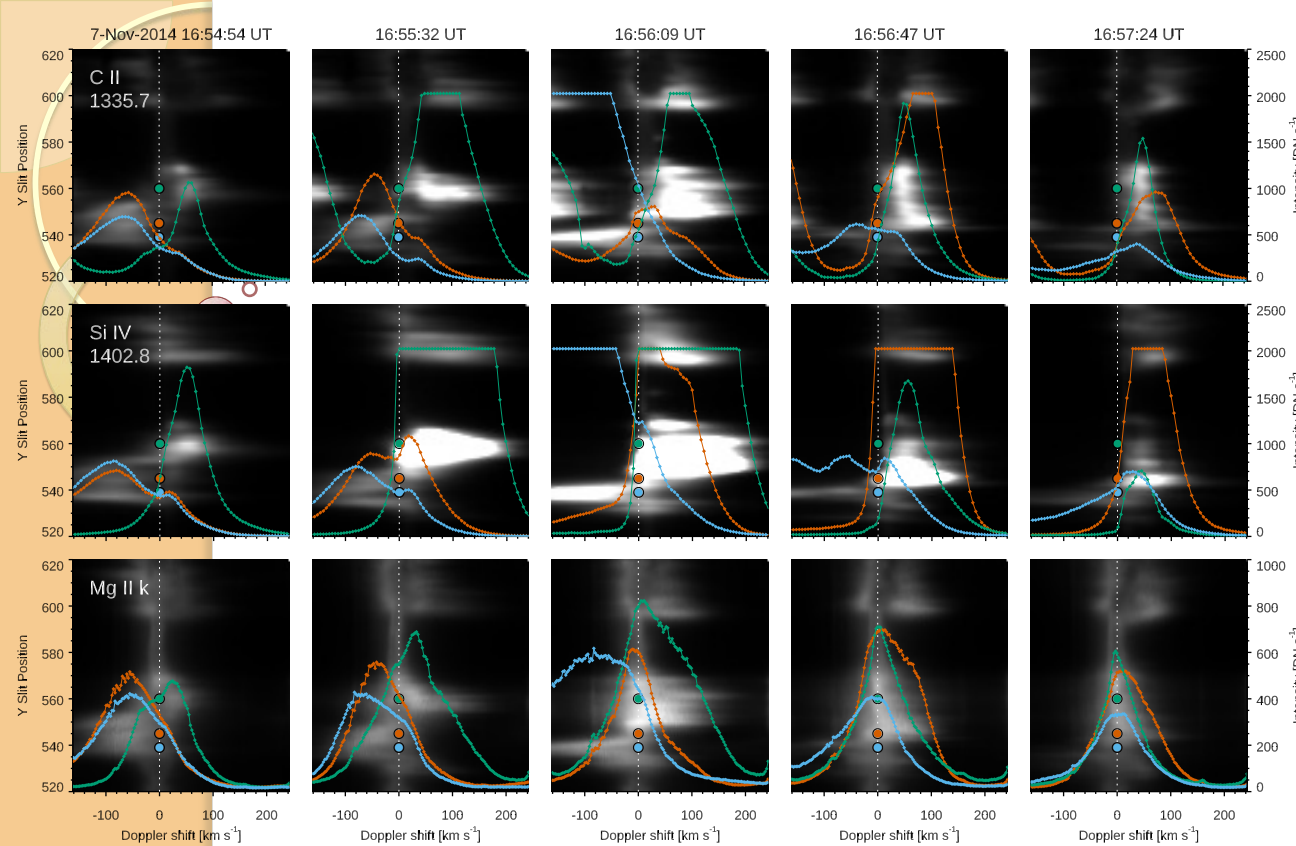


NUV



- **Blue line:** average intensity in five of the IRIS spectral ranges in the pixels at raster position (3,[537:539]) at 16:56:47 UT
- **Orange line:** same as blue line, for raster position (3,[543:545])
- **Green line:** same as blue line, for raster position (3,[558:560])
- **Black line:** average intensity calculated at the same time along 20 consecutive slit positions (from 160 to 179), corresponding to a **quiet-Sun region**.

Note that the blue curve exhibits a **very prominent bump** in the blue wing of the Si IV @ 1402.8 Å line, and in the blue wings of the C II @ 1334 and 1336 Å, and Mg II h and k lines.



Line profiles for three different pixel positions of the IRIS slit for C II 1335.75 Å (top row), Si IV 1402.8 Å (middle row) and Mg II k 2796.31 Å (bottom row).

In each row the line profiles for successive times are overplotted on the relevant spectrograms. The dashed vertical lines indicate the position of the line center (laboratory rest wavelengths), while the colored circles show the slit position relevant to the profiles indicated with the same colors.

❑ For selected time intervals and slit positions, the line profiles of **C II** and **Si IV** (IRIS dataset) indicate **blueshifts followed by redshifts**, while the **Mg II k** line profile indicate that **at the same time but in different pixel positions**, blueshifts and redshifts are present.

❑ Two possible scenarios:

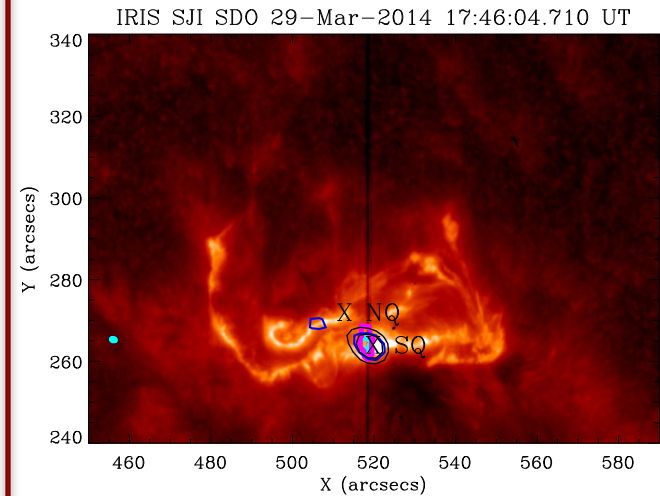
- ❖ **chromospheric evaporation followed by condensation**
- ❖ **the blueshifts are actually indicative of the rising motion of a flux rope observed in AIA images.**

Sunquakes: how can flare energy propagate towards the solar interior ?

- *Sunquakes: seismic waves observed for some but not all CMEs and M- and X-class flares (Kosovichev & Zharkova, 1998; Donea, 2011).*

These waves refract through layers deep in the convection zone and appear as surface ripples, traveling at speeds of some tens of km s^{-1} .

They have energy between 10^{27} and 10^{29} erg and come from a source with an area of the order of 10 Mm^2 (associated with HXR and WL sources).



Matthews et al., ApJ 2015

If the flare energy is released in the corona, in order to drive an acoustic disturbance in the solar interior, the energy must propagate through nine pressure scale heights.

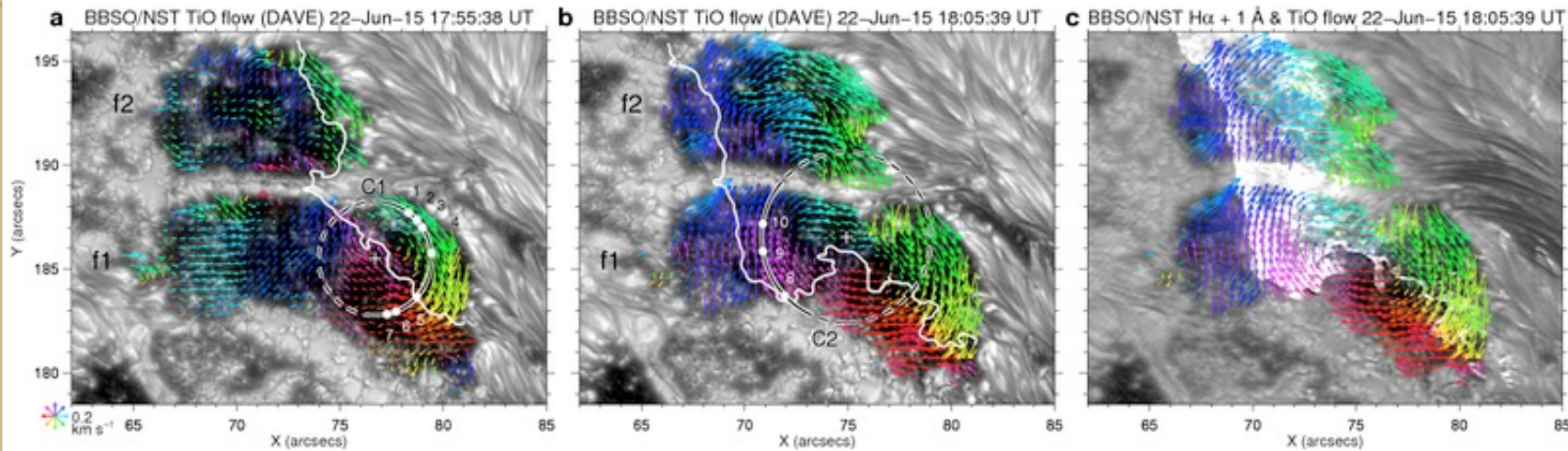
Changes of the photospheric magnetic field during/after flares

Sudol & Harvey (2005) studied 20 major flares observed between 1999 and 2005, and found *evidence of longitudinal magnetic field changes* in 15 X-class flares.

They concluded that “*one of the basic assumptions of flare theories, that the photospheric magnetic field does not change during flares, needs to be reexamined.*”

Rapid magnetic changes in the course of major flares were also observed in *horizontal magnetic fields* (*Schmieder et al. 1994; Wang et al. 1994, Wang 2007*).

Flare-induced Impulsive Sunspot Rotation caught in High Resolution

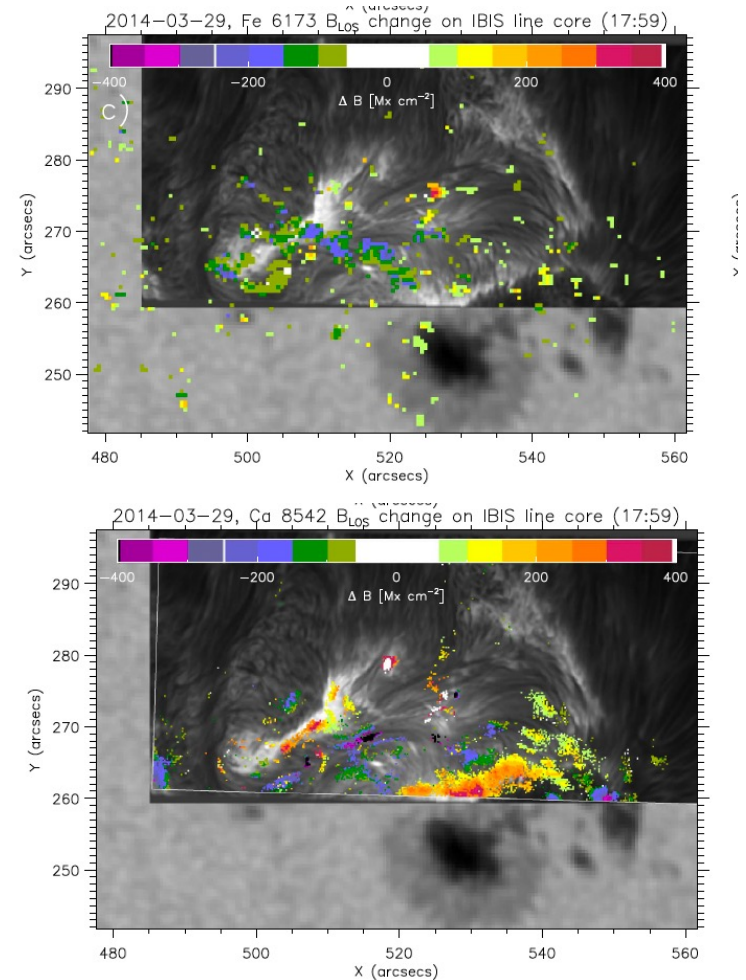


*RHESSI Science nugget
(November 2016) Chang Liu
et al.*

See also Anwar et al. 1993

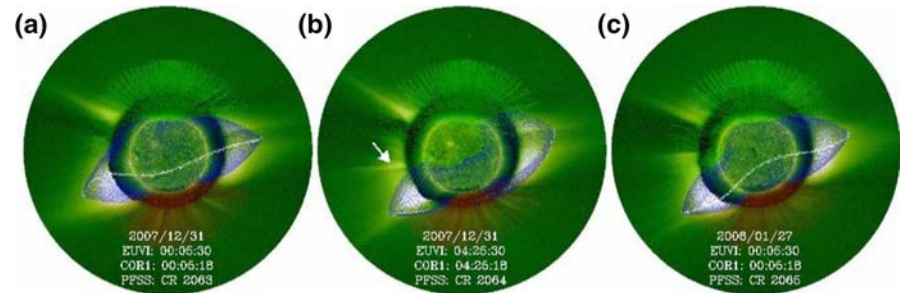
Changes of the Chromospheric magnetic field during flares

- Changes of the chromospheric B_{LOS} during an XI-flare on 2014 March 29. These are stronger (maximum value 640 Mx cm^{-2}) and in larger areas than the photospheric changes.
- Photospheric changes are located near the polarity inversion line, chromospheric changes seem to predominantly occur near the footpoints of coronal loops.
- Changes are near (a few arcsec), but not perfectly co-spatial with HXR emission. Enhanced AIA emission occurs in nearly all locations that show changes of the magnetic field.



Coronal Mass Ejections

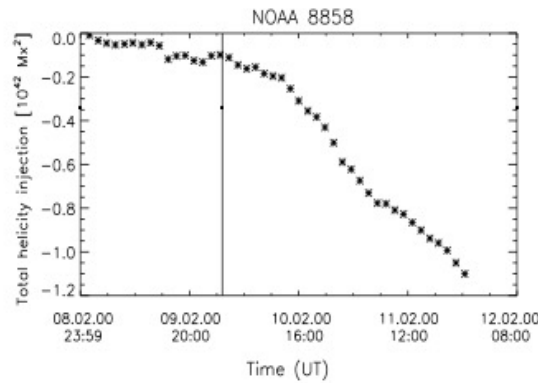
CMEs can cause important changes and reconfiguration of the (coronal) magnetic field, i.e., displacements of helmet streamers and shrinkage of coronal holes.



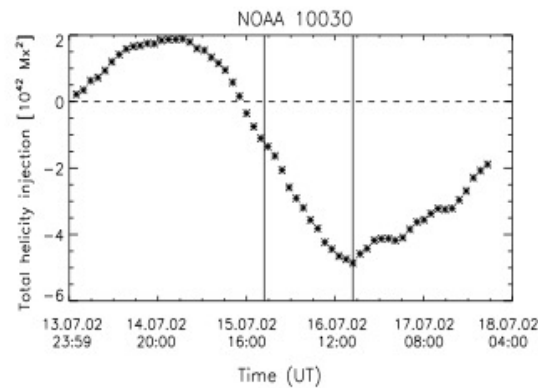
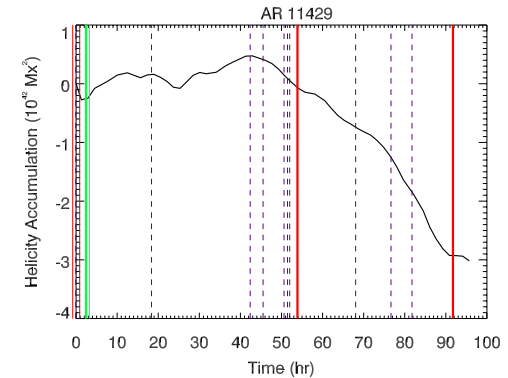
Due to a CME, the coronal streamer migrated southwards, and then persisted for more than one solar rotation.

- ❖ CMEs can reduce the coronal magnetic helicity, carrying during their travel an amount of $\sim 10^{41} - 10^{43} \text{ Mx}^2$.
- ❖ During flares not associated to CMEs, magnetic helicity cannot be efficiently dissipated, so that magnetic helicity in the corona will be continuously buildup.

Trend of magnetic helicity before and after CMEs

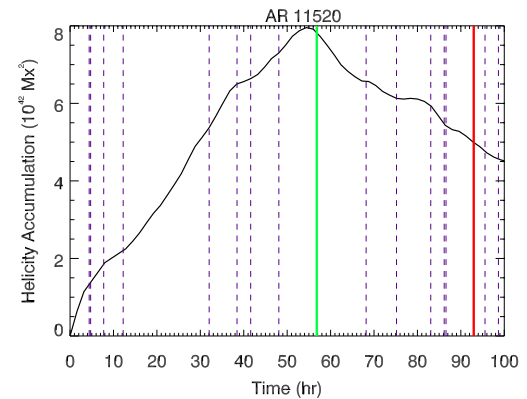
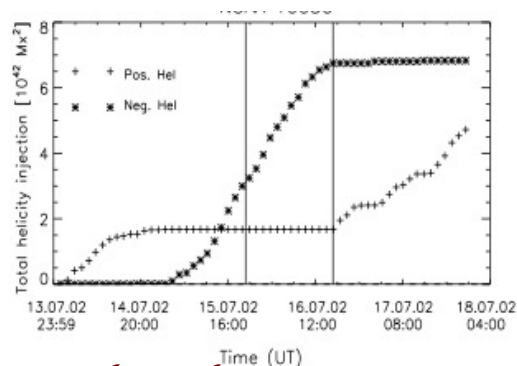
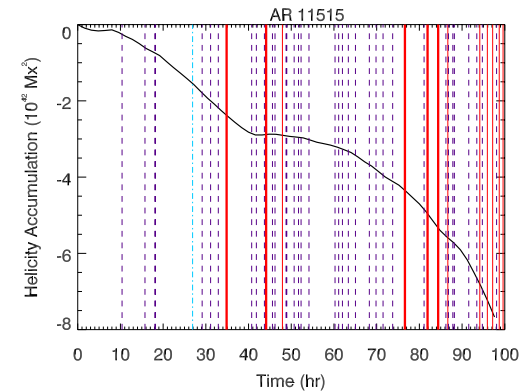


Park et al. (2010) showed that in flaring ARs the helicity injection was twice that of non-flaring regions.



However, it is not possible to single out a general rule on the behaviour of the magnetic helicity after a CME, as it can:

- continue to grow
- start to decrease
- become constant,
- change its sign.



Correlation between Flares - Eruptive Filaments - CMEs

- More than 80% of (filament) eruptions lead to CMEs (Schmieder et al. 2013).
- The energy threshold for near one-to-one correspondence between flares and CMEs appears to be at the GOES X2 level (Hudson, 2010).

Authors	Number of CMEs	Period	CMEs associated with eruptive prominences	CMEs associated with H α flares
St. Cyr and Webb (1991)	73	1984 – 1986	76 %	26 %
Gilbert et al. (2000)	18	1996 – 1998	76 %	94 %
Subramanian and Dere (2001)	32	1996 – 1998	59 %	
Zhou, Wang, and Cao (2003)	197	1997 – 2001	94 %	88 %

TABLE 6.2: Correlation between CMEs and flares for CDAW and CACTus datasets in the \pm two hours time interval.

Flares		CDAW		CACTus	
GOES class	Number of events	flare associated with CME \pm 2 h [%]	CMEs not associated with flares [%]	flare associated with CME \pm 2 h [%]	CMEs not associated with flare [%]
C	17,712	10003 (56.47 %)	11074 (48.40 %)	7755 (43.78 %)	6396 (41.22 %)
M	1884	1308 (69.43 %)		1242 (65.92 %)	
X	155	130 (89.39 %)		121 (78.06 %)	

TABLE 6.3: Correlation between CMEs and flares for CDAW and CACTus datasets in the \pm one-hour time interval.

Flares		CDAW	CACTus
GOES class	Number of events	flare associated with CME \pm 1 h [%]	flare associated with CME \pm 1 h [%]
C	17,712	5842 (32.98 %)	4228 (23.87 %)
M	1884	951 (50.48 %)	771 (40.92 %)
X	155	118 (76.13 %)	86 (55.48 %)

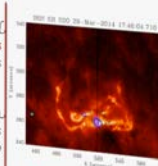
TABLE 6.4: Correlation between CMEs and flares for CDAW and CACTus datasets in the \pm 30 min. time interval.

Flares		CDAW	CACTus
GOES class	Number of events	flare associated with CME \pm 30 min. [%]	flare associated with CME \pm 30 min. [%]
C	17,712	2992 (16.89 %)	2159 (12.19 %)
M	1884	445 (23.62 %)	341 (18.099 %)
X	155	62 (40.00 %)	37 (23.87 %)

Open questions

Sunquakes: how can flare energy propagate towards the solar interior?

Sunquakes are seismic waves that are observed for some but not all coronal mass ejections (CMEs) and M- and X-class flares (Kova, 1998; Donati, 2011).

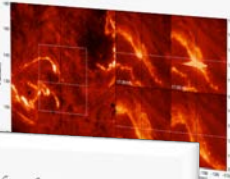


Matthews et al., *ApJ* 2015

acoustic wave typically has an ν and 10^{20} erg and comes an area of the order of 10^8 km².

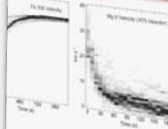
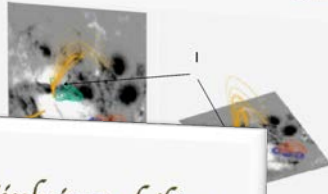
energy is released in the corona, in order to drive an acoustic wave towards the solar interior, the energy must propagate through nine orders of magnitude of plasma, magnetic field conditions on flare energy

in flaring loop:



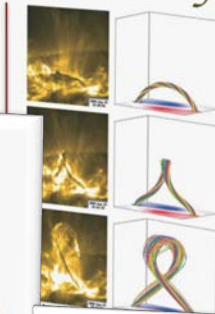
- SOL20140910 (PRIS, SDO)
- X1.6 flare in NOAA-12158
- One ribbon moves down, spectrometer slit (Fe XXI ~ 10 MK)
- Velocity profiles obtained at 80 pixels along the PRIS slit

Null points and hard X-ray sources



Kink instability

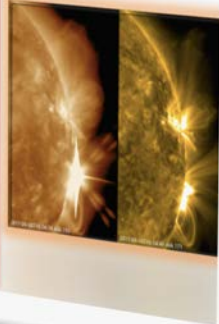
A flux tube twisted beyond a certain critical limit becomes unstable



SD1 magnetogram: intrusion, while the SS42 'HT' (blue), is triaxial.

What triggers the eruption?

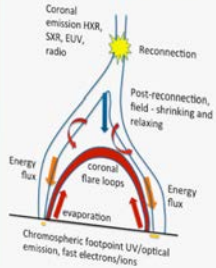
- Magnetic reconnection
- Exceeding of a threshold (magnetic gradient, shear angle, height of the flux rope, accumulated magnetic helicity, ... magnetic field configuration, ...)



The paradigm of the magnetic coupling of the solar atmosphere

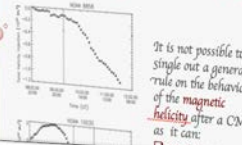
The main question of flare physics is to understand:

- How the energy, previously stored in a stressed coronal magnetic field, is released so rapidly,
- transported through the atmosphere of the Sun,
- converted into the kinetic energy of the non-thermal particles and thus, or otherwise, into the flare's radiation output.



Fletcher, 2014

2 rules of magnetic helicity before and after CMEs



It is not possible to single out a general rule on the behaviour of the magnetic helicity after a CME, as it can:

- Emergence of magnetic bundles (and frozen-in plasma)
- Horizontal motions of the photospheric plasma at loop footpoints ($\sim 10^4$ W m⁻²)

Magnetic energy storage

Potential (current-free) magnetic field
 $\nabla \times \vec{B} = 0$

Force-free magnetic field
 $\nabla \times \vec{B} = \alpha \vec{B}$

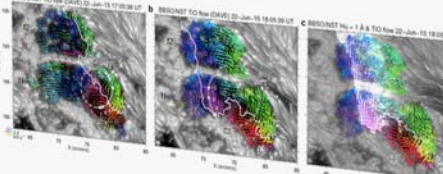
- DISSSIPATION
- Current sheets (magnetic field and plasma are locally decoupled) \rightarrow reconnection
 - $l \sim 100 - 1000$ km
 - $l \sim 10^2 - 10^3$ min
 - $l \sim 20$ Mm (from models of RR)
 - Not all the free energy is released

Coronal mass Ejections

CMEs (expulsion of mass of the order of $10^{17} - 10^{18}$ kg)



Flare-induced Impulsive Sunspot Rotation caught in High Resolution

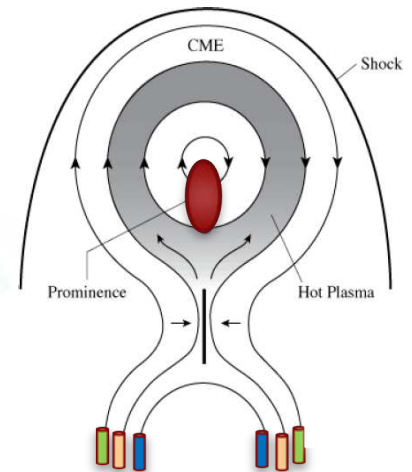
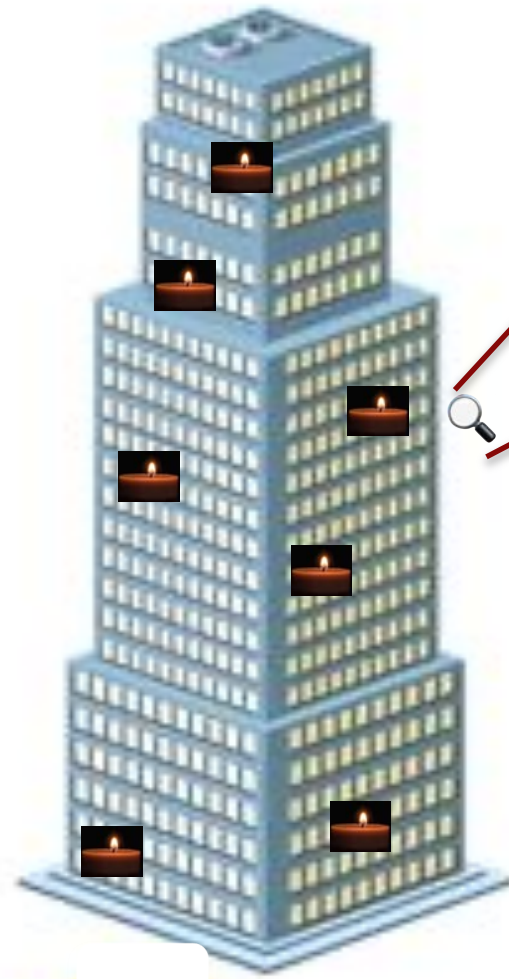
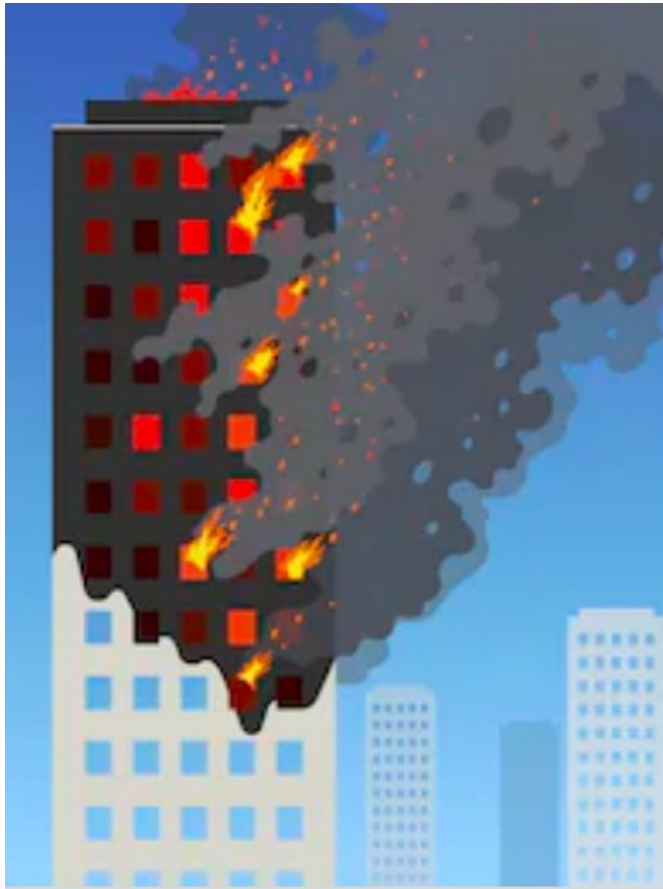


RHESSI Science Magnetogram (November 2016) Chang Liu et al.

streamer migrated southwards, to share one solar rotation.

carrying during their ... in the corona reveal a ... hemisphere and a negative ... magnetic helicity cannot be ... in the corona will be

Eruptive events: we need to know where, when and how the magnetic energy is stored and released



WE NEED HIGH RESOLUTION OBSERVATIONS



Thanks for your attention